STUDY OF THE RADIOLYTIC ENHANCEMENT OF GOLD NANOPARTICLES WITH AMINO ACIDS

An Undergraduate Research Scholars Thesis

by

MALLORY ELAINE CARSON

Submitted to Honors and Undergraduate Research
Texas A&M University
in partial fulfillment of the requirements for the designation as an

UNDERGRADUATE RESEARCH SCHOLAR

Approved by
Research Advisor: Dr. Gamal Akabani

May 2015

Major: Radiological Health Engineering

TABLE OF CONTENTS

Page

ABSTRACT

Study of the Radiolytic Enhancement of Gold Nanoparticles with Amino Acids. (May 2015)

Mallory Elaine Carson
Department of Nuclear Engineering
Texas A&M University

Research Advisor: Dr. Gamal Akabani
Department of Nuclear Engineering

Gold nanoparticles have become a growing field of study in cancer diagnosis and treatment. Several articles have shown that gold nanoparticles have the capacity to enhance the absorbed dose in localized tissue; however, consistent studies of their reported enhancement are scarce. Amino acids, a major constituent of human cells and tissue, were used as a model for assessing dose enhancement. In the current study, twenty aqueous amino acids with and without PEGylated and non-functionalized 5 nm gold nanoparticles were prepared and irradiated to 10 kGy, 25 kGy, and 50 kGy using a 10 MeV electron beam and analyzed using UV-VIS spectrophotometry. A semi-quantitative response to conformational changes as a function of absorbed dose for radiosensitive amino acids following the Arrhenius equation was summarized and compared to samples containing gold nanoparticles. Inclusion of any nanoparticles provided only 0.01 - 0.04 increase in absorbance universally; thus for the low concentrations used in this experiment, radiolytic enhancement and differences in optical density caused by gold nanoparticles are grossly indeterminate. While enhancement has been previously shown to be achievable through the addition of small gold nanoparticles in *in vitro* and *in vivo* studies, other considerations such as nanoparticle size and concentrations may need to be modified to indicate such difference.

DEDICATION

This thesis is lovingly dedicated to my family and friends. I wish to express special thanks to my parents Mitchell and Karen Carson, who have continually inspired me to have courage pursue my dreams, no matter the size. My brother Matthew has also encouraged and loved me in ways only a sibling can. This thesis is also dedicated to my dearest friends, who have supported me without end. I will always appreciate the inspiration and support, especially Jacob Glenn for the countless hours spent reading and providing feedback and Daniel San Miguel for providing personal reassurance in my work. May God bless you all.

ACKNOWLEDGEMENTS

I would like to extend my deepest appreciation to Dr. Gamal Akabani for becoming my research mentor and constantly pushing me toward continued learning and success. He offered exceptional insight and knowledge into this project and educated me on how to become an independent researcher. I would also like to thank Jijie Lou for her assistance in laboratory procedures and advice concerning amino acid chemistry. Many thanks to the Undergraduate Summer Research Grant Program at Texas A&M University for providing personal funding and enabling me to explore my interests through extensive research. Lastly, thanks to the Undergraduate Research Scholars program for providing me the opportunity and training to write a thesis as an undergraduate student in preparation for further studies.

NOMENCLATURE

AuNP	Gold nanoparticle
PEG	Polyethylene glycol
PEG-AuNP	PEGylated gold nanoparticle
ROS	Reactive oxygen species
UV-VIS	Ultraviolet-visible

CHAPTER I

INTRODUCTION

1.1 Purpose of the study

The purpose of this study is to characterize the radiolytic effects caused by the addition of gold nanoparticles (AuNPs), bare and PEGylated, to isolated amino acid solutions. For this investigation, amino acids serve as a basic model for biological systems, considering their integral role in the function of such systems. By employing amino acids, the extent to which AUNPs interact in a physical manner through radiolysis is observed. UV-VIS spectrophotometry presents the consequences of irradiation at the molecular level, namely to qualify the possible radiolytic enhancement via AuNPs and to illustrate nanoparticle agglomeration in solution.

The implications of this study are far-reaching: by eliminating several biological factors such as enzymatic reactions, protein denaturation, and biochemical actions or pathways, amino acids may serve as a reasonable model for true dose assessment. Furthermore, the mechanisms by which nanoparticles interact with amino acids and their radiolytic products may be applied to their interactions with peptides and proteins. Through these evaluations it may then be possible to better predict and determine the effectiveness of radiotherapies utilizing functionalized or non-functionalized AuNPs.

1.2 Effects of radiation on biological systems

Radiobiology, a discipline involving the interaction of ionizing radiation with living systems, is a subject of great importance in the understanding of natural cellular processes as well as current

applications such as cancer therapies and diagnostics. Two different processes are involved in the biologic effects of radiation: (1) direct ionization along charged particle tracks and (2) the indirect effects caused by the generation of free radicals and other entities that diffuse away from ionization tracks [1]. This second set is dominant in inducing intracellular damages and is typically in the form of reactive oxygen species (ROS) derived from the radiolysis of water.

The creation and effects of ROS can result in both beneficial and deleterious outcomes *in vivo*. In low concentrations, ROS can be involved in mediating cellular signaling pathways and maintaining homeostasis. In greater concentrations, ROS can induce chromosomal aberrations, DNA base alterations, and the cleavage of peptide bonds in proteins [1, 2]. Cellular DNA damages are greatly cytotoxic, as radiation-induced mutations are believed to be a strong factor in cell viability. Radical reactions with proteins and amino acids themselves may also induce modifications that alter cellular functions by inactivating enzymes or directly altering or degrading protein structures.

Typically cells contain antioxidants and free radical scavengers to protect against extensive radiolysis. However, these protections are inherently limited based on the balance between ROS production and the cell's capability to mitigate its effects. Recovery may be possible if the incident radiation is minimal, but for higher doses radiolysis can induce significant biological changes which are beyond repair.

Yet the biological effects of radiation can be exploited advantageously. In more recent applications like cancer treatment, an increased yield of ROS can enhance the oxidative stress in

a tumor cell and result in apoptosis [1]. While much is understood in the overall biological effects of radiolysis, there is still more to be discovered in its molecular modalities. Studying the radiolysis of amino acids, peptides, and proteins is paramount in further understanding cellular dynamics under irradiation.

1.3 Introduction to amino acids

Amino acids are organic compounds consisting of carboxyl (COOH) and amino (NH_2) functional groups, accompanied by a side-chain unique to the species. Amino acids can be classified in a variety of ways: side-chain composition (aliphatic, aromatic, sulfur-containing, etc.), polarity, pH, and functional group locations. Those whose functional groups are located at the first carbon are denoted as α-amino acids and are integral to biochemistry. Common classifications for these amino acids are summarized in Table 1.1.

Table 1.1. Classifications of amino acids (with abbreviations) based on R-group composition

Hydrophobic Aliphatic		**Hydrophobic Aromatic**		**Polar Neutral Side Chain**	
Alanine	Ala	Phenylalanine*	Phe	Asparagine	Asn
Glycine	Gly	Tryptophan*	Trp	Glutamine	Gln
Isoleucine*	Ile	Tyrosine	Tyr	Serine	Ser
Leucine*	Leu			Threonine*	Thr
Proline	Pro				
Valine*	Val				
Acidic		**Basic**		**Sulfur-containing**	
Aspartic Acid	Asp	Arginine	Arg	Cysteine	Cys
Glutamic Acid	Glu	Histidine*	His	Methionine*	Met
		Lysine*	Lys		

* indicates essential amino acid

The twenty standard amino acids, which are also all L-stereoisomers, are a major constituent of human cells and other tissues, being only second to water in composition. Of these, nine are

labeled as “essential” (shown in Table 1.1) because humans cannot synthesize them directly. All standard amino acids are directly involved in protein synthesis via peptide bonds, hence their common designation as the “building blocks” of proteins. Some amino acids are also responsible for the regulation of metabolic pathways, growth, development, hormone synthesis, and reproduction [3]. In order to achieve proper protein and biomolecule synthesis, as well as provide energy for multiple cellular processes, amino acids must remain balanced in the body.

Protein synthesis is achieved because of the complex chemistry of amino acids. Amino acids exist interchangeably as zwitterions containing a positive ammonium group and negative carboxylate group. This state facilitates the nucleophilic addition/elimination reaction necessary to create a peptide bond as the oppositely-charged groups come in proximity. Such bonds can be made in series to form polypeptide chains as precursors to proteins.

Should the balance of amino acid compositions be offset, entire body homeostasis can be disturbed or even cause death. For example, tyrosine and tryptophan are important precursors to neurotransmitters like dopamine and other catecholamines. Previous studies by Hinz et al. have shown a direct connection between these amino acids and neurological disorders like Parkinson’s disease and depression due to L-DOPA and serotonin imbalance [4]. Optimal treatment of Parkinson’s disease with L-DOPA required the careful balance of tyrosine, tryptophan, and cysteine due to their subsequent depletion from the therapy [4]. Another condition, tyrosinemia, occurs when tyrosine cannot be properly metabolized, resulting in conditions such as acute liver disease and kidney damage [5]. This enzyme deficiency is typically accounted for through diets

low in tyrosine and phenylalanine, which can be converted into tyrosine [5]. The proper administration of amino acids is vital to maintaining health and treating disease.

Amino acids are also significant in their ability to serve as predictors of disease. It has been demonstrated that the metabolic signatures of tyrosine, phenylalanine, and isoleucine can indicate diabetes and cardiovascular disease development [6]. With so many cellular functions and other diseases characterized by amino acid availability, knowing how these biomolecules are affected by radiation can provide insight into the maintenance of biological systems.

1.4 Fundamentals of radiolysis

Radiolysis in its most general sense is the disassembly and modification of molecules by ionizing radiation. This dissociation of one or more chemical bonds can lead to subsequent chemical interactions in the surrounding medium. In biological systems, the radiolysis of water is of great relevance because it is the greatest constituent of living things and its exposure can have significant consequences. The mechanism for the radiolysis in water follows three stages: (1) the physical stage of radiation absorption causing ionization or excitation, (2) the physicochemical stage in which unstable products dissipate energy through various processes, and (3) the chemical stage during which species react and diffuse throughout the solution [7]. When exposed to radiation, water molecules dissociate into various forms following radical termination and oxygen saturation [8]:

$$H_2O \rightarrow \bullet OH,\ e_{aq}^{-},\ H\bullet,\ O_2^{\bullet -},\ H_2O_2,\ H_2 \qquad (1.1)$$

Reactive oxygen species (ROS) such as H_2O_2 and assorted oxygen compounds release excessive amounts of energy when converting back into more stable states in aqueous solutions [7]. The

yields of these products when formed by low-LET radiation depend on several factors including pH, absorbed dose, and dose rates.

Radical species in water are generally short-lived but largely reactive. The physical stage is achieved 1 fs after initial radiation interaction and leads to the formation of ionized water molecules and electrons [7]. The physicochemical stage (10^{-15} - 10^{-12} s) allows for ion-molecule reactions, autoionization, and thermalization of electrons [7]. During the chemical stage (10^{-12} - 10^{-6} s) the radiolytic products diffuse throughout branched tracks, depositing energy in the medium through reactions and thermalization [7].

Energy from ionizing particles is not distributed uniformly, but rather in packages called spurs [8]. A spur can contain multiple free-radical pairs, which may interact with one another, causing subsequent exchanges and diffusion [8]. Under densely ionizing radiation, spurs in close proximity may form tracks that can branch off with increasing effects through radical reactions. The self-termination of these radicals often proceeds by the following forms [8]:

$$\bullet OH + e_{aq}^{-} \rightarrow \bullet OH \quad (1.2)$$

$$\bullet OH + H \rightarrow H_2O \quad (1.3)$$

$$2 \bullet OH \rightarrow H_2O_2 \quad (1.4)$$

$$2H\bullet \rightarrow H_2 \quad (1.5)$$

$$2e_{aq}^{-} + 2\ H^{+} \rightarrow H_2 \quad (1.6)$$

As described previously, when ROS and radicals are created, they diffuse throughout the solution and interact with other entities in the medium. Primary radiolytic products of water react with target molecules in solution. Hydrogen abstraction results from the reaction of H• or •OH to

form a solute radical, R•, which is believed to be a cause of substantial damage in biological molecules [8]. Dissociation reactions liberate entire functional groups (e.g. amides, carboxylic acids, etc.) on organic compounds. Addition reactions combine radicals together or radicals and non-radicals. Solute radicals formed may also react with each other or with other reactants to form stable products by dimerization, additions of oxygen, or hydrogen transfer [8]. To determine specific products for a given solute would require further investigation and the complete characterization of reaction mechanisms.

1.5 Radiolysis of amino acids

Under normal physiological conditions, amino acids can undergo oxidation via ROS and become involved in biological functions. The radiolysis of amino acids has been a subject of study in the past, but never has a comprehensive study been accomplished. Currently it is known that much of radiolysis is mediated via the radiolytic products of water; thus, they may typically follow the mechanisms for target molecules as described previously.

Studies by Hatano have elucidated much of these effects through the analysis of several α-amino acids. Based on the constant ammonia yield over a range of irradiation doses, it was supposed that deamination is caused by aqueous radiolytic products while part of an amino acid is directly oxidized by radiation [9]. More studies on peptides and proteins suggested similar mechanisms and the following interactions from organic free radicals [10]. It was found that peptide bonds were broken under γ-irradiation, yielding free amino acids, residues, and recombinations [10].

More research efforts support this work by demonstrating the possible dimerization and cross-linking of amino acids and proteins [2, 11]. Milligan et al. established that amino acid residues in DNA-binding proteins may be able to reverse DNA oxidation or form cross-links that could inhibit repair [12]. It has been postulated that the mechanism of the radiolysis of peptides and proteins is linked to the mechanisms proposed for the reaction of amino acids [13]. By studying amino acids in the context of radiolysis, it may be possible to infer how intracellular protein structures are affected by radiation and thus better understand the consequences of irradiation *in vivo*.

1.6 Gold nanoparticles in biological applications

Recently, gold nanoparticles (AuNPs) have become a subject of comprehensive study in biomedical applications. AuNPs are attractive in nanomedicine research because they are considered to be biologically inert, producing few cytotoxic effects [14]. Moreover, they possess a number of desirable characteristics including controllable size and shape during synthesis and surface chemistry, indicating their possible multifunctionality for *in vivo* applications [15, 16].

AuNPs exhibit localized surface plasmon resonance (LSPR); this optical property makes them highly useful in surface enhanced Raman spectroscopy (SERS) or enhanced contrast in MRI [15-17]. AuNPs are also being studied in-depth because of their ability to conjugate with polyethylene glycol (PEG-SH) and other sulfhydryl-terminated substrates via thiol linkages [18]. These functionalization moieties have been shown to increase colloidal stability and biocompatibility of nanoparticles [18, 19]. They also slow clearance rates *in vivo* and to allow

for the conjugation of antibodies for targeted cell therapy, given some cancer cells tend to overexpress certain membrane antigens, leading to preferential uptake [16, 20, 21].

Given the increased use of AuNPs in medicine, it is relevant to study the effects of these nanoparticles when used in external beam radiotherapy, brachytherapy, and nuclear medicine oncology [22-26]. Previous studies have demonstrated that the use of small AuNPs (≤ 5 nm) in aqueous solutions increases the generation of ROS during irradiation [26]. This process is two-fold: the first process is associated with the direct interactions of ROS generated in water with the surface of the gold nanoparticles, and the second process is due to a direct interaction of photons and high-energy electrons with gold nanoparticles resulting in the production of a cascade of Auger electrons.

The first *in vivo* demonstration of malignant tumor control using AuNPs was performed by Hainfield et al. The injection of small AuNPs prior to irradiation increased the survival rate in tumor-bearing mice significantly (86% long-term survival, compared to 20% for irradiation alone) [27]. In this experiment and others following it, the enhanced permeability and retention (EPR) effect of leaky vasculature in tumors is attributed to the maximal uptake of AuNPs, and the presumed preferential absorption of x-rays by AuNP constitutes much of its therapeutic effects through photoelectron emission [25, 27].

It has been suggested that functionalized and non-functionalized AuNPs can enhance the radiosensitivity of tumors through the preferential absorption of x-rays and interactions with the surrounding media [20, 27]. However, direct comparison of the radiolytic efficacies of these two

forms is scarce. The potential enhancement of ROS by AuNP interactions may have a significant effect on the radiolysis of water and amino acids. Therefore it is necessary to evaluate the extent of these physical interactions to corroborate the hypotheses posed in previous studies and justify the use of nanoparticles in radiotherapies.

1.7 Atomic Theory of UV-VIS spectrophotometry

Optical spectroscopy is based on the Bohr-Einstein frequency relationship for photon energies in Equation 1.1,

$$\Delta E = h\nu \tag{1.1}$$

where h is Planck's constant and ν is the frequency of light [28]. This relationship directly links the atomic or molecular energy states with the frequency of electromagnetic radiation used to induce excitement. When atoms or molecules absorb electromagnetic radiation, they are transformed from a ground state into an excited state. In this process, energies of specific wavelengths are absorbed within the molecular bonds, and these electrons are promoted to higher energy orbitals. This is to state that photons of a given frequency will be preferentially absorbed for a specific bond because the energy required to transition to a higher energy state is precisely the energy provided by the impinging photons. However, these promotions are dependent on the bond structures between atoms; typically electrons in a non-bonding or π orbital move to the π* antibonding molecular orbital [29]. Because standard UV-VIS spectrophotometers typically work in the wavelength range of about 200 nm (in the near UV region) to about 800 nm (in the very near IR region), only a limited number of energy transitions may be possible, thus leading to the preferential absorption in some bond types.

For light produced by a spectrophotometer, photons may be absorbed by the molecules in the medium, leading to a decreased intensity of light at the end of the path length, or transmitted through [28]. The amount of interaction between the observed solution and light depends on the molecular configuration and concentration in solution. Light intensities and molar concentration for a given wavenumber ν (wavelength λ) may be related according to the Beer-Lambert law in Equation 1.2:

$$\log\left(\frac{I_0}{I}\right)_\nu = \log\left(\frac{100}{T(\%)}\right)_\nu = A = \varepsilon \cdot c \cdot d \tag{1.2}$$

where A is the absorbance, T is the transmittance, I_0 is the intensity of the monochromatic light entering the sample, I is the intensity of light emerging from the sample, ε is the molar absorptivity coefficient, c is the concentration of the light-absorbing material, and d is the path length of the sample [28]. By this relation one can directly relate the concentration of a chemical species in solution to the relative absorbance of light based on its characteristic electron excitations. This relation is typically only valid for low concentration solutions, as high concentrations increase interactions between solute molecules and can change several properties of the molecules, including light attenuation [28].

However, if promotion in electronic states was the only interaction involved in the absorption of ultraviolet or visible light, one would expect an absorption spectrum to contain discrete points at different wavelengths. Instead, the specific energies required for these transitions may appear as a continuum due to modulations in the rotational and vibrational states of a molecule [28]. These interactions continually change the energies of the orbitals, leading to absorption over a range of wavelengths. Other interactions that may decrease the resolution of a peak in an absorbance spectrum include the delocalization of pi bonds through conjugation and solvent properties,

including polarity, pH, temperature, or other interferences. The UV transmission of solvents depends critically upon the solvent purity, so this variable, as well as those previously listed, must be controlled or accounted for in order to identify and characterize the substances present in a solution [28, 30]. Because of these interactions, molecules are often characterized by a parameter λ_{max}, the wavelength at which maximum absorption occurs.

Typical applications of UV-VIS spectrophotometry include determining the molar absorptivity or concentration of a pure solute in solution, in accordance with the Beer-Lambert law. Note that this practice is most often reserved for pure solutions; mixtures can be analyzed, but only if it is known that the components do not interfere greatly with the absorptions of other constituents and all individual properties are known. This is of great importance considering that absorption is an additive process. For pure substances, the wavelengths of absorption peaks may be correlated with the types of bonds in a given molecule; this idea proves essential in determining the functional groups within a molecule. Quantitatively, UV-VIS spectrophotometry is a tool for the estimation of the amount of a compound in a sample.

UV-VIS spectrophotometry is also used as a qualitative tool to better identify and interpret the physicochemical properties of a species. For example, absorbance can be changed depending on the molecule's state of protonation (a function of the solution pH). Often this can be observed as a shift in the peak value. For this reason, unless solubility demands acidic or basic conditions, neutral conditions may be preferred for observation. Delocalization of bonds and changes in bond structures following interactions may also cause shifts in the maximum absorption. Lastly,

the identity of the chemical may be confirmed through its absorbance properties when UV-VIS techniques are used in conjunction with other analytical methods.

For organic compounds, UV-VIS spectrophotometry may provide excellent insight for their intrinsic properties and roles in biological mechanisms. Under some physical or chemical interactions, functional groups may be produced or altered, yielding information regarding possible interaction mechanisms. For amino acids specifically, detection generally requires the absorbance of the carboxyl group (-COOH), which exhibits absorbance in the 200 to 210 nm range, as well as aromatic rings in the 250 to 280 nm range [31]. Any alterations experienced by these prominent molecular features would certainly express detectable changes in the absorption spectra.

CHAPTER II

METHODS AND MATERIALS

2.1 Amino acid sample preparation

All chemicals were used as received from Sigma Aldrich with purity >99.9% and used without further purification. Stock solutions were produced by dissolving solid amino acids in deionized water (ELGA PURELAB Flex) at 0.1 M, excluding aspartic acid, glutamic acid, tryptophan, and tyrosine, whose concentrations were 0.03 M, 0.05 M, 0.05 M, and 0.002 M, respectively due to hydrophobicity. All solutions were stored at 4°C when not in use.

Non-functionalized standard 5 nm gold nanoparticles (9.08E-8 M) in 0.1 mM phosphate-buffered saline were obtained from CytoDiagnostics (Burlington, Ontario). 1 mL solutions for each amino acid were produced by combining 0.1 mL of the standard AuNP solution with 0.9 mL of the amino acid solution, yielding solutions with a 9.08E-9 M nanoparticle concentration. Solid mPEG-SH (MW 2000) was obtained from Layson Bio, Inc. (Arab, Alabama). PEGylated nanoparticles (PEG-AuNP) were produced by combining an aqueous solution of 0.01 M mPEG and standard 5 nm AuNP solution in a 3000:1 molar ratio (according to reported molarities) to ensure proper decoration [32]. The resultant solution was agitated for 2 hours and left to set for more than 12 hours to complete the PEGylation process. No further processing was performed. For each amino acid, 1 mL solutions were produced by combining 0.1 mL of the PEG-AuNP solution with 0.9 mL of the aqueous amino acid solution, yielding an 8.84E-9 M nanoparticle concentration. It is assumed that interaction between mPEG and amino acid will be trivial due to

the low concentrations used in this experiment and because the hydrophilicity of the amino acid produces a repulsive interaction with PEG in solution [33].

2.2 Electron beam irradiation

Irradiations of all solutions were carried out at the National Center for Electron Beam Research (NCEBR) at Texas A&M University. The planned absorbed doses in these studies were selected at 10, 25, and 50 kGy. Alanine dosimetry methods were used to assess the actual absorbed dose to the irradiated samples: the free radical formed by alanine is very stable and yields a dose-dependent electron paramagnetic resonance (EPR) signal. Alanine pellets irradiated with the samples were analyzed with a Bruker e-scan Alanine Dosimetry System. The actual delivered doses were approximately 0, 10.56, 28.61, and 53.92 kGy. Because of limited available quantities of the solutions, these samples were irradiated in 1.5 mL microcentrifuge tubes in which they were originally prepared to ensure no volume loss. While this presented a level of error in absorbed dose from varying geometry and air space, such effects were expected to be only ± 2 kGy for any given volume of solution. Effects of polypropylene degradation in the tubes were assumed negligible.

2.3 UV-VIS spectrophotometry

A NanoDrop 2000c UV-VIS spectrophotometer (Thermo Scientific) was used to evaluate the absorbance spectra of all amino acid solutions. Previous studies with organic matter have successfully utilized UV-VIS spectrophotometry to measure radiation response [34-36]. All measurements were carried out using the 2 μL pedestal on the device. Deionized water was used as a blank reference. Given that absorbance is proportional to path length, it was deemed

necessary after initial tests to use the spectrophotometer pedestal for measurement with a nominal path length of 1 mm instead of cuvette measurements due to the possibility of high absorbance obscuring results. Baseline correction for all spectra was developed at 750 nm under the assumption that no absorbance should occur at this wavelength. The reported concentration of the standard AuNP solution (9.08E-8 M) was verified by UV-VIS spectrophotometry using measured absorbance and the reported molar extinction coefficient in accordance with the Beer-Lambert law.

CHAPTER III

RESULTS

3.1 Pure amino acid solutions

To clearly determine how the addition of nanoparticles affects the radiolysis of amino acids, it was first necessary to study the amino acids in isolation. Because each has a unique molecular composition and structure, the radiolytic processes in these solutions cannot be truly generalized. In order to determine which amino acids could serve as a means of observing dose enhancement (as different amino acids can exhibit varying radioresistance), all twenty amino acids were irradiated and analyzed with UV-VIS spectrophotometry.

Prior to irradiation, all solution samples appeared clear with no precipitates or residues present. An overview of observed results for pure amino acids is presented in Table 2.1 with reference to recorded spectra in the Appendix. All UV-VIS spectra were collected between 220 nm to 400 nm. Due to the high absorbance of mPEG near 200 nm, data in the shorter UV range are omitted from analysis.

Little changes were evident in water, both qualitatively and in UV-VIS absorbance. This behavior was expected, as radicals produced in water are short-lived (10^{-12} - 10^{-6} seconds) and its molecular state is very stable [7]. Few visible changes post-irradiation were noted in the other solutions, excluding histidine and tryptophan, which drastically changed color. Histidine turned yellow and became darker with increasing dose, and tryptophan became orange-red similarly, both of which are to be attributed to the production of chromophores as residues. Phenylalanine,

threonine, and tyrosine exhibited slight yellowing with no other significant changes. Cysteine and methionine developed sulfurous odors possibly due to the liberation of hydrogen sulfide. All irradiated samples exhibited a strong pungent odor due to the liberation of ammonia.

Table 1.1. UV-VIS responses to radiation of pure amino acid solutions. Figures are presented in the Appendix.

Figure Number	Solution	UV-VIS Spectrophotometry Observations
A1	Water	No significant observations
A2	Alanine	No significant observations
A3	Arginine	Peak broadening at 220 nm; marginally higher absorbance with dose
A4	Asparagine	New absorbance band at 276 nm increases in intensity with dose
A5	Aspartic Acid	Minor increases in absorbance as function of dose
A6	Cysteine	Minor increases in absorbance as function of dose
A7	Glutamic Acid	Minor increases in absorbance as function of dose
A8	Glutamine	Increasing absorbance and flattening between 250 nm and 320 nm with dose
A9	Glycine	Minor increases in absorbance as function of dose
A10	Histidine	New absorbance band at 282 nm depicts strong increase in intensity with dose
A11	Isoleucine	No significant observations
A12	Leucine	No significant observations
A13	Lysine	Minor flattening-out effect with dose
A14	Methionine	Increasing absorbance and flattening between 270 nm and 315 nm with dose
A15	Phenylalanine	Increasing intensity and minor right-ward shift of peaks from 223 nm and 258 nm; absorbance increases universally as function of dose
A16	Proline	No significant observations
A17	Serine	Broadening and increased absorption evident as function of dose
A18	Threonine	Broadening and increased absorption evident as function of dose
A19	Tryptophan	Peak broadening and increased absorption from 299 nm to 380 nm
A20	Tyrosine	Minor peak shift and broadening from 275 nm to 284 nm with dose
A21	Valine	No significant observations

The analysis of the UV-VIS spectra as a function of absorbed dose was carried out based on amino acid functional groups as described previously in Table 1.1. For some amino acid samples, the absorbance intensity of a given wavelength was exponentially related to absorbed dose, which suggested that radiolytic reactions of amino acids followed first order kinetics as established by the Arrhenius equation, as Eq. 3.1:

$$A = A_{max}(1 - \exp(-D/D_0)) + A_0 \quad (3.1)$$

where A_0 is the initial absorbance at zero absorbed dose, D_0 is the absorbed dose required to increase the absorbance A by 37%, and A_{max} is the maximum increase in absorbance produced by irradiation. The fit was established by selecting wavelengths at which little or no absorption was evident in the control sample (0 kGy) and the dose response appeared consistent with no strong shifting. Among all amino acids, nine displayed excellent fit to this exponential saturation (Fig. 3.1), indicating this model's plausibility. Asparagine and methionine seem to better approximate linear trends in the dose range studied, but generally, saturation better reinforces the physical limitations of radical formation in solution.

In considering the amino acid classifications, the observations from UV-VIS can be summarized. There were no observable changes in UV-VIS spectra for aliphatic amino acids. Likewise, acidic amino acids did not present strong changes. Aromatic amino acids showed increasing absorbance as a function of absorbed dose and minor right-ward peak shifts. Neutral amino acids yielded new absorbance bands increasing with intensity with absorbed dose. Basic amino acids displayed mixed results: lysine showed no observable changes in its UV-VIS spectrum; however, arginine showed peak broadening at 220 nm, and histidine displayed a new absorbance band at 282 nm

with a strong increase with absorbed dose. Lastly, sulfur-containing amino acids showed increases in absorbance as a function of absorbed dose, as well as increases in sulfurous odors.

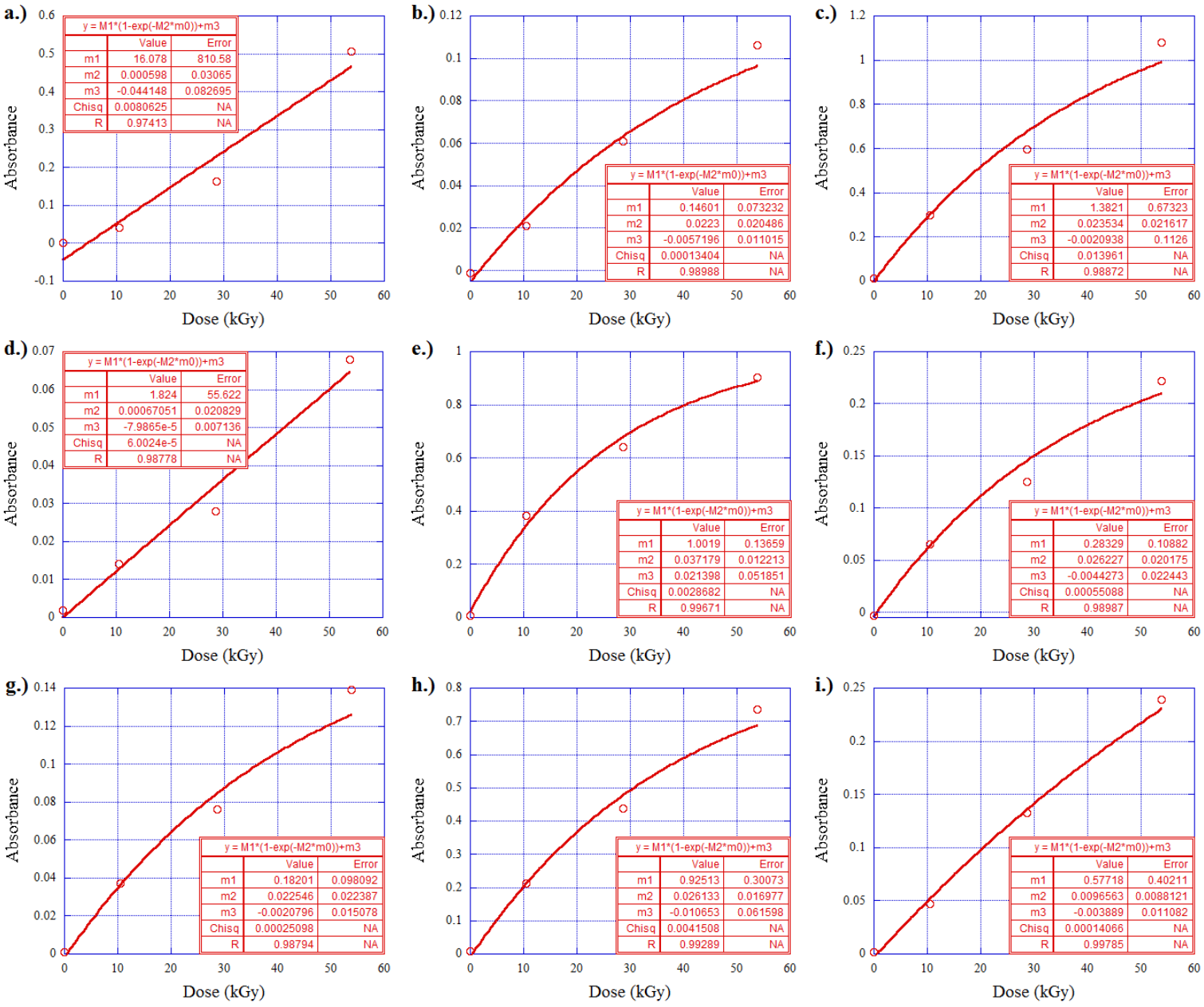

Figure 3.1. Dose-to-absorption response curves for a) asparagine at 278 nm, b) glutamine at 280 nm, c) histidine at 282 nm, d) methionine at 298 nm, e) phenylalanine at 278 nm, f) serine at 280 nm g) threonine at 260 nm, h) tryptophan at 320 nm, i) tyrosine at 305 nm.

3.2 Amino acids with AuNPs

Most solutions retained a transparent pink hue when initially combined with AuNPs and PEG-AuNPs (which typically appear red), implying neither aggregation nor significant amino acid-AuNP interactions occurred. However, some solutions experienced visible changes with bare AuNPs: prior to irradiation, small black agglomerations appeared in cysteine while aspartic acid and glutamic acid turned faintly purple, all of which indicate the presence of nanoparticle aggregation. This behavior is reasonable because these amino acids are the most acidic with isoelectric point (pI) values of 5.02, 2.98, and 3.08, respectively. It has been previously determined by Zakaria, et al. that pH, especially concerning increased acidity, plays a significant role in nanoparticle agglomeration, so the presence of aggregation prior to irradiation is justified [37]. These aggregations were then exacerbated with increasing dose as residues were produced. Much of these aggregations were not, however, observed when PEG-AuNP was combined with the amino acid solutions.

Despite 5 nm AuNPs having a characteristic peak absorbance at 520 nm, changes in nanoparticle structure post-irradiation were not discernible via UV-VIS due to the low concentration used (this peak was not observable due to the magnitude difference between AuNP signal and that of the remaining solution). Visible changes were still evident: arginine, glutamine, methionine, and proline also showed some forms of aggregation post-irradiation, as these solutions became clear and displayed dark purple/black residues. However, while some solutions with PEG-AuNP lost color, only cysteine experienced any significant aggregation with PEG-AuNP. This demonstrates that overall PEGylation was performed correctly and was sufficient to prevent surface

interactions between the amino acid and nanoparticle. Because of its singularity, cysteine's interaction is presumed to be mediated by its sulfhydryl group.

Of those that exhibited significant changes in relation to dose, comparisons between the pure sample and those with functionalized and non-functionalized nanoparticles were grossly indeterminate. Solutions with nanoparticles achieved higher absorption than the isolated solutions universally (as displayed in Figures A1 - A21 in the Appendix), but there is no significant relation, for additions in absorbance were slight (ranging 0.01 - 0.04) when compared to the magnitude of optical density presented for each solution. For UV-VIS spectrophotometry, mixtures create additive absorbance, so the minor increases in absorbance may be attributed simply to the natural absorption of AuNPs, as this same range is expressed in control solutions of water (Fig. A1). PEGylated and bare nanoparticle differences were very slight due to similar absorbance values. Dose response relationships shown by three species in Fig. 3.2 also indicate little change between these groups and the isolated amino acids. If radiolytic enhancement is considerable in reality, it is trivial for the variables acknowledged in the current study, which include, but are not limited to, concentration, nanoparticle size, and irradiation method.

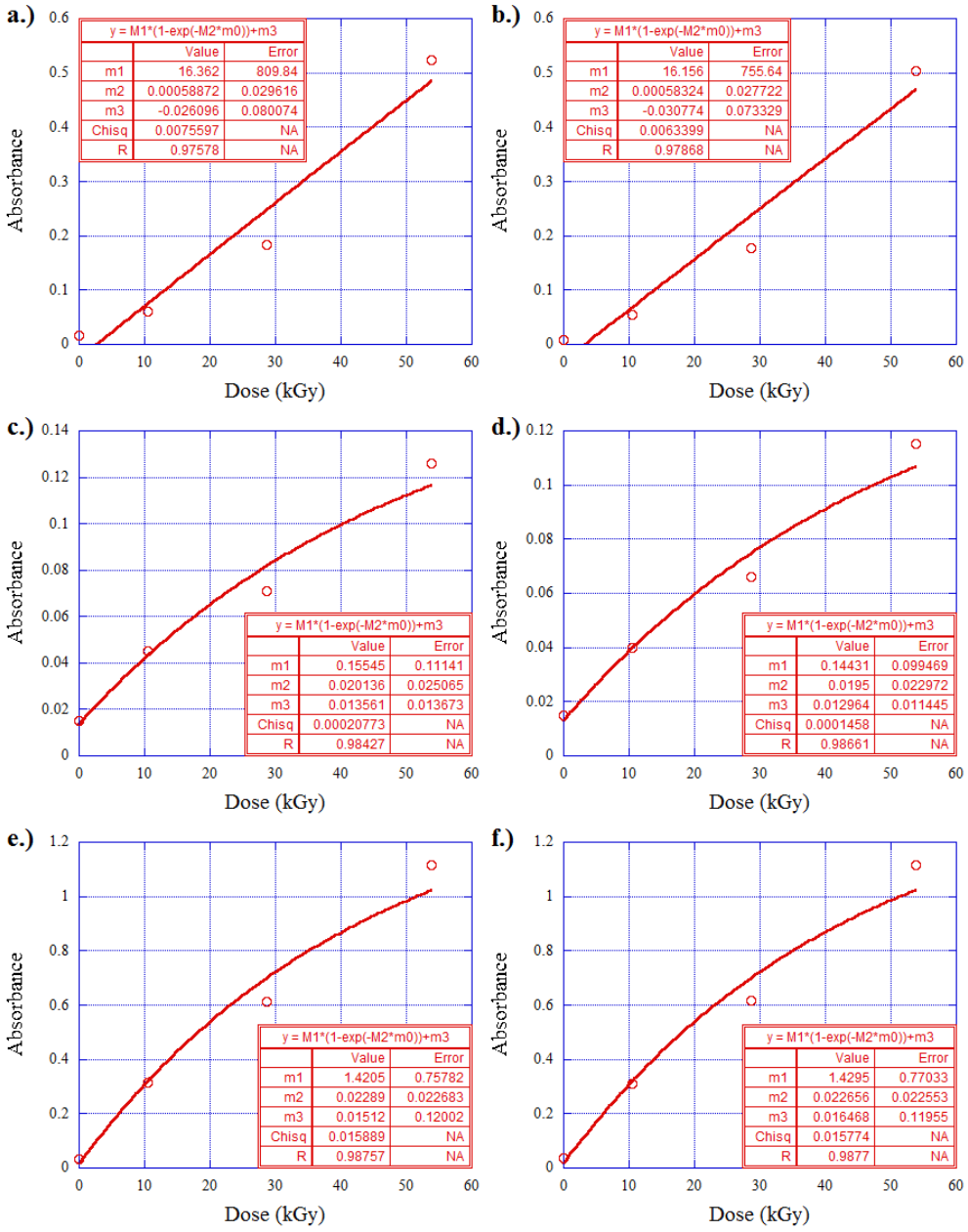

Figure 3.2: Dose-to-absorption response curves for a.) asparagine with bare AuNP at 278 nm, b.) asparagine with PEG-AuNP at 278 nm, c.) glutamine with bare AuNP at 280 nm, d.) glutamine with PEG-AuNP at 280 nm, e.) histidine with bare AuNP at 282 nm, f.) histidine with PEG-AuNP at 282 nm.

CHAPTER IV

DISCUSSION

4.1 Radiolytic product interpretation

For asparagine and histidine, the creation of a new absorption band is indicative of a stable residue (or combination of similar residues) that exhibit preferential formation under radiolysis, as the peak position is constant and increases in intensity with dose. Minor peak shifting experienced by phenylalanine and tyrosine may suggest pH variations, which can affect the absorption spectra of organic compounds and therefore must be taken into account [28]. Flattening or broadening of spectra are signs of inhomogeneities in solution and may indicate a wider distribution of radiolytic products. The presence of dissimilar species in solution also presents divergence from the conventional Beer-Lambert law. While differences in composition can be accounted for, it is necessary to know the species being formed. Therefore further analysis needs to be completed to better characterize the identities of these residues and the resultant solution properties.

Regardless of encountered discrepancies, several pure solutions remained clear and experienced little change regardless of dose. These observations suggest certain amino acids exhibit stronger radioresistance and/or stability. In fact, alanine has been widely used in electron spin resonance dosimetry because of these properties: when irradiated in the solid state, alanine undergoes deamination and produces a very stable alkyl free radical that can be accurately measured to determine absorbed dose. With this understanding it may be possible to use other amino acids as indicators should the radiolytic products be characterized.

In this experiment hydrophobic aliphatic and acidic amino acids show no significant response to dose, whereas hydrophobic aromatic, polar neutral, and basic amino acids exhibited greater responses. Therefore, the molecular structure may play a significant role in the radiosensitivity of the amino acid, possibly presenting favored interactions. Oxidation by ROS is presumed to be the dominant interaction in the cleavage of amino acid, so knowing which substrates are susceptible to oxidation is useful in determining these radiolytic processes and products.

Sulfurous odors were observed in cysteine and methionine, which demonstrates that oxidation may occur preferentially at groups containing sulfur. Hatano established that the radiolysis of cysteine liberated its sulfhydryl group in both small and large radiation exposures, and these experiments confirmed the group's increased sensitivity to oxidation caused by the ROS [38]. As demonstrated previously, these observations are of great interest in the determination of protein denaturation and destruction, as sulfhydryl liberation has been found in enzyme proteins [38]. Thus the characterization of a hydrogen sulfide product in irradiated cysteine is supported as a favorable interaction.

Other residue structures may be hypothesized based on spectral observations and ongoing research. Increasing absorbance in the longer wavelength regions may indicate a distribution of products of higher molecular weight. To achieve this in pure solutions, there must be some oxidation and recombination of side chain amino acid radicals or additional radiolytic products. Previous studies have shown that the formation of dipeptides and cross-linking are possible under irradiation; these events can be measured and extended to the radiolysis of proteins [2, 11].

It is possible that these products may exist in small concentrations in the solutions irradiated in this experiment.

4.2 Saturation relationships

The relationship between absorbance and radiation dose in aqueous amino acids with and without nanoparticles has been shown to generally follow an Arrhenius equation. This data trend corroborates with earlier studies by Rotblat and Simmons who measured five crystalline amino acids via microwave spectroscopy and demonstrated similar responses after exposure to electron beam irradiation [39]. While those studied were not the same species that showed relationships for this experiment, it can be noted that this relationship may hold true regardless of state. Differences in response from may be derived from solvent interactions as well as the method of measurement. The dose-absorption relationships of solutions containing nanoparticles were also shown not to vary drastically from isolated samples, suggesting that the presence of AuNP, at least for the concentration presented in the current study, did not greatly affect the identities or extent of residues generated by irradiation.

4.3 Nanoparticle interactions

Due to the indiscernibility of AuNPs in individual UV-VIS spectra, only observable interactions are noted for these purposes. AuNP aggregations appearing only post-irradiation were not evident in all solutions, but those amino acids that expressed evidence did so in more than one dose. It is thus proposed that aggregations were induced by interaction with the resultant solution, though the mechanism by which aggregation occurred is unknown. As stated before,

pH may be a probable cause, as well as the chemical characteristics of amino acid residues. Amino acids may either provide a site of reaction or protection from agglomeration.

Cysteine is a singularity in that it was the only amino acid to show unique forms of aggregation on the PEG-AuNP solutions. This interaction is greatly presumed to be mediated by the substitution of the thiol linkage in PEG-SH, as sulfur has a high binding affinity to gold. It may then be postulated that cysteine has the possibility to decorate AuNP because of its side-chain composition, or that the sulfhydryl group liberated during irradiation may have replaced PEG-SH and exposed the nanoparticle surface to interactions otherwise prevented by the presence of PEG.

In considering the effects of AuNPs on the UV-VIS spectra, the small recorded increase in absorption overall for those solutions containing either functionalized or non-functionalized AuNPs indicates little in terms of the efficacy of small nanoparticles for radiolytic enhancement under the present conditions. Further considerations need to be made to decipher the true cause for the little change observed, possibly through the modulation of AuNP concentration, nanoparticle size, or administered dose.

4.4 Experimental limitations

The limitations of this study may elucidate methods by which research with amino acids and AuNPs may be improved. Overall this experiment was extremely limited by the concentration of AuNPs used. No significant differences or distinct nanoparticle signals could be discerned in UV-VIS spectra because the concentration was below the threshold of observability. Nevertheless, radiolytic enhancement is still a possibility. While these experimental solutions

contained nanomolar concentrations of AuNP, previous *in vitro* and *in vivo* studies showing success in dose enhancement varied from nanomolar to millimolar [40]. In this regard it is evident that increasing the concentration of nanoparticles may have led to quite different observations and a more definitive conclusion.

Yet such disparity raises the question of what conditions are most appropriate to observe dose enhancement. The aforementioned successes relied on an assortment of variables including nanoparticle size, surface functionalization, irradiation method, and cell lines or models used in addition to nanoparticle concentration. Nanoparticle size and radiation beam energies can also correlate for maximum efficacy, which may undermine the reliability of the results presented here, since only one particle size and one beam energy were considered. Biological mechanisms may also play a role in determining the efficacy, considering ROS production and cell radiosensitivity. Also, Butterworth, et al. determined that actual dose enhancements reported by these studies were much greater than those predicted by Monte Carlo methods [40]. Despite small nanoparticles being considered efficient energy carriers, considerable concentrations are still necessary to observe dose enhancement, and correlations between these variables are questionable. Considering these factors together it is difficult to generate viable conclusions based on the data of previous studies other than that radiosensitization was present to some degree. Overall, the experiments reported here are intended to be much more basic and provide a more direct approach to assessing the actual dose enhancement of AuNPs in biological systems.

CHAPTER V

CONCLUSION

In the current study, twenty amino acids in solution were combined with functionalized and non-functionalized AuNPs and irradiated to 10, 25 and 50 kGy by 10 MeV electron beam and subsequently analyzed using UV-Vis spectrophotometry. It was found that a causal relationship exists between absorbed dose and UV-VIS response in amino acids. This relationship can be successfully modeled by the Arrhenius equation to explain the nature of radical production during irradiation. While not all samples demonstrated significant saturation response, observable patterns in UV-VIS absorbance in several amino acids can be attributed to the formation of stable residues either as radicals or recombination products. Therefore structure and functionality are strong determinants of how amino acids conform under radiolysis.

While some solutions differed physically with functionalized and non-functionalized AuNPs, absorbance values increased only slightly in comparison to pure amino acids. The same dose relationships were determined for these samples and remained relatively unmodified from the controls. Despite nanoparticle aggregations occurring in several samples before and after irradiation, the overall effects of these phenomena were indeterminate. With greater classification and understanding of the amino acid radiolytic products, it may be possible to better interpret AuNP interaction mechanisms.

While nanoparticle-mediated dose enhancement has been previously claimed through *in vitro* and *in vivo* studies, this assertion is not substantiated by the present study. No significant

enhancement and changes in dose response relationships were observed by either bare or PEGylated nanoparticles. Because greater success has been shown in biological models, it is suggested that the radiosensitization property of AuNPs may be more correctly determined by other factors, including biological processes and cell sensitivity, rather than simply physical interactions. These observations do not discount the medicinal applications of AuNPs, but rather they elucidate the predominant mechanism of AuNP interaction in living systems. Even so, there are several issues that need to be addressed, such as nanoparticle size and radiation energy correspondence, in order to determine the validity of this claim.

Overall, because there exists a plethora of factors to be considered in the analysis of nanoparticle efficacy under irradiation, further research should be conducted to isolate the greatest contributing factors to dose enhancement in biological systems. Pertinent factors including surface chemistry, particle size, concentrations, and radiation sources should be addressed in an isolated manner to determine their distinct biological effects. With this research accomplished, it may be possible to generate combinatorics to provide certain desired efficacies.

The overarching purpose of this study is to cast a wide net in discerning radiolytic enhancement of gold nanoparticles by using amino acids as a basic molecular model. While these results remain inconclusive concerning the nature of nanoparticle interactions, it may be possible to expand upon this basis as previously suggested to better conclude the extent of dose enhancement with small gold nanoparticles.

REFERENCES

1. Selman, J., *Elements of Radiobiology*. 1983: C.C. Thomas.

2. Stadtman, E.R. and R.L. Levine, *Free radical-mediated oxidation of free amino acids and amino acid residues in proteins.* Amino Acids, 2003. **25**(3-4): p. 207-218.

3. Wu, G., *Amino acids: metabolism, functions, and nutrition.* Amino acids, 2009. **37**(1): p. 1-17.

4. Hinz, M., A. Stein, and T. Uncini, *Amino acid management of Parkinson's disease: a case study.* International journal of general medicine, 2011. **4**: p. 165.

5. Kitagawa, T., *Hepatorenal tyrosinemia.* Proceedings of the Japan Academy. Series B, Physical and biological sciences, 2012. **88**(5): p. 192.

6. Magnusson, M., et al., *A diabetes-predictive amino acid score and future cardiovascular disease.* European heart journal, 2012: p. ehs424.

7. Le Caër, S., *Water radiolysis: influence of oxide surfaces on H2 production under ionizing radiation.* Water, 2011. **3**(1): p. 235-253.

8. Lehnert, S., *Biomolecular action of ionizing radiation.* Biomolecular Action of Ionizing Radiation. Series: Series in Medical Physics and Biomedical Engineering, ISBN: 978-0-7503-0824-3. Taylor & Francis, Edited by Shirley Lehnert, 2007. **1**.

9. Hatano, H., *Studies on Radiolysis of Amino Acids and Proteins II. On Radiolytic Deamination of Amino Acids in Aqueous Solutions by Gamma Irradiation.* Journal of Radiation Research, 1960. **1**(1): p. 28-37.

10. Hatano, H., *Studies on Radiolysis of Amino Acids and Proteins III. On Radiolysis of Peptides and Proteins in Aqueous Solutions by Gamma Irradiation.* Journal of Radiation Research, 1960. **1**(1): p. 38-45.

11. Uvaydov, Y., N.E. Geacintov, and V. Shafirovich, *Generation of guanine-amino acid cross-links by a free radical combination mechanism.* Physical Chemistry Chemical Physics, 2014. **16**(23): p. 11729-11736.

12. Milligan, J., et al., *Repair of oxidative DNA damage by amino acids.* Nucleic acids research, 2003. **31**(21): p. 6258-6263.

13. Wheeler, O.H., *Radiolysis of peptides and proteins.* Photochemistry and Photobiology, 1968. **7**(6): p. 675-681.

14. Lewinski, N., V. Colvin, and R. Drezek, *Cytotoxicity of nanoparticles.* Small, 2008. **4**(1): p. 26-49.

15. Lim, Z.-Z.J., et al., *Gold nanoparticles in cancer therapy.* Acta pharmacologica Sinica, 2011.

16. Boisselier, E. and D. Astruc, *Gold nanoparticles in nanomedicine: preparations, imaging, diagnostics, therapies and toxicity.* Chemical Society reviews, 2009. **38**(6): p. 1759-1782.

17. Toma, H.E., et al., *The coordination chemistry at gold nanoparticles.* Journal of the Brazilian Chemical Society, 2010. **21**: p. 1158-1176.

18. DeLong, R.K., et al., *Functionalized gold nanoparticles for the binding, stabilization, and delivery of therapeutic DNA, RNA, and other biological macromolecules.* Nanotechnology, science and applications, 2010. **3**: p. 53.

19. Zhang, X.-D., et al., *Size-dependent radiosensitization of PEG-coated gold nanoparticles for cancer radiation therapy.* Biomaterials, 2012. **33**(27): p. 6408-6419.

20. Chattopadhyay, N., et al., *Design and characterization of HER-2-targeted gold nanoparticles for enhanced X-radiation treatment of locally advanced breast cancer.* Molecular pharmaceutics, 2010. **7**(6): p. 2194-2206.

21. Etame, A.B., et al., *Design and potential application of PEGylated gold nanoparticles with size-dependent permeation through brain microvasculature.* Nanomedicine: Nanotechnology, Biology and Medicine, 2011. **7**(6): p. 992-1000.

22. Chanda, N., et al., *Radioactive gold nanoparticles in cancer therapy: therapeutic efficacy studies of GA-198AuNP nanoconstruct in prostate tumor-bearing mice.* Nanomedicine : nanotechnology, biology, and medicine, 2010. **6**(2): p. 201-209.

23. Douglass, M., E. Bezak, and S. Penfold, *Monte Carlo investigation of the increased radiation deposition due to gold nanoparticles using kilovoltage and megavoltage photons in a 3D randomized cell model.* Medical Physics, 2013. **40**(7): p. 071710.

24. Ngwa, W., et al., *In vitro radiosensitization by gold nanoparticles during continuous low-dose-rate gamma irradiation with I-125 brachytherapy seeds.* Nanomedicine : nanotechnology, biology, and medicine, 2013. **9**(1): p. 25-27.

25. Hainfeld, J.F., et al., *Gold nanoparticles enhance the radiation therapy of a murine squamous cell carcinoma.* Physics In Medicine And Biology, 2010. **55**(11): p. 3045-3059.

26. Misawa, M. and J. Takahashi, *Generation of reactive oxygen species induced by gold nanoparticles under x-ray and UV Irradiations.* Nanomedicine : nanotechnology, biology, and medicine, 2011. **7**(5): p. 604-614.

27. Hainfeld, J.F., D.N. Slatkin, and H.M. Smilowitz, *The use of gold nanoparticles to enhance radiotherapy in mice.* Physics in medicine and biology, 2004. **49**(18): p. N309.

28. Perkampus, H.-H., H.C. Grinter, and T. Threlfall, *UV-VIS Spectroscopy and its Applications*. 1992: Springer.

29. Clark, B., T. Frost, and M. Russell, *UV Spectroscopy: Techniques, instrumentation and data handling*. Vol. 4. 1993: Springer.

30. Misra, P. and M.A. Dubinskii, *Ultraviolet spectroscopy and UV lasers*. 2002: CRC Press.

31. *Analytical Methods of Amino Acids*. Shimadzu Corporation 2014; Available from: http://www.shimadzu.com/an/hplc/support/lib/lctalk/53/53intro.html.

32. Liu, Y., et al., *Synthesis, stability, and cellular internalization of gold nanoparticles containing mixed peptide-poly (ethylene glycol) monolayers.* Analytical chemistry, 2007. **79**(6): p. 2221-2229.

33. Sasahara, K. and H. Uedaira, *Solubility of amino acids in aqueous poly (ethylene glycol) solutions.* Colloid and Polymer Science, 1993. **271**(11): p. 1035-1041.

34. Nakano, H., et al., *Change in the UV-VIS Absorbance of Amino Acids as a Result of Femtosecond Laser Irradiation.* Journal of Laser Micro/Nanoengineering, 2007. **2**(1): p. 100.

35. Yordanov, N. and Y. Karakirova, *Sugar/UV spectrophotometric system for high-energy dosimetry (0.055–160kGy).* Radiation measurements, 2007. **42**(1): p. 121-122.

36. Salah, N., et al., *Functionalization of gold and carbon nanostructured materials using gamma-ray irradiation.* Radiation Physics and Chemistry, 2009. **78**(11): p. 910-913.

37. Zakaria, H.M., et al., *Small Molecule-and Amino Acid-Induced Aggregation of Gold Nanoparticles.* Langmuir, 2013. **29**(25): p. 7661-7673.

38. Hatano, H., *Studies on radiolysis of amino acids and proteins I. On radiolytic oxidation of sulfhydryl groups.* Journal of Radiation Research, 1960. **1**(1): p. 23-27.

39. Rotblat, J. and J. Simmons, *Dose-response relationship in the yield of radiation-induced free radicals in amino acids.* Physics in medicine and biology, 1963. **7**(4): p. 489.

40. Butterworth, K.T., et al., *Physical basis and biological mechanisms of gold nanoparticle radiosensitization.* Nanoscale, 2012. **4**(16): p. 4830-4838.

APPENDIX

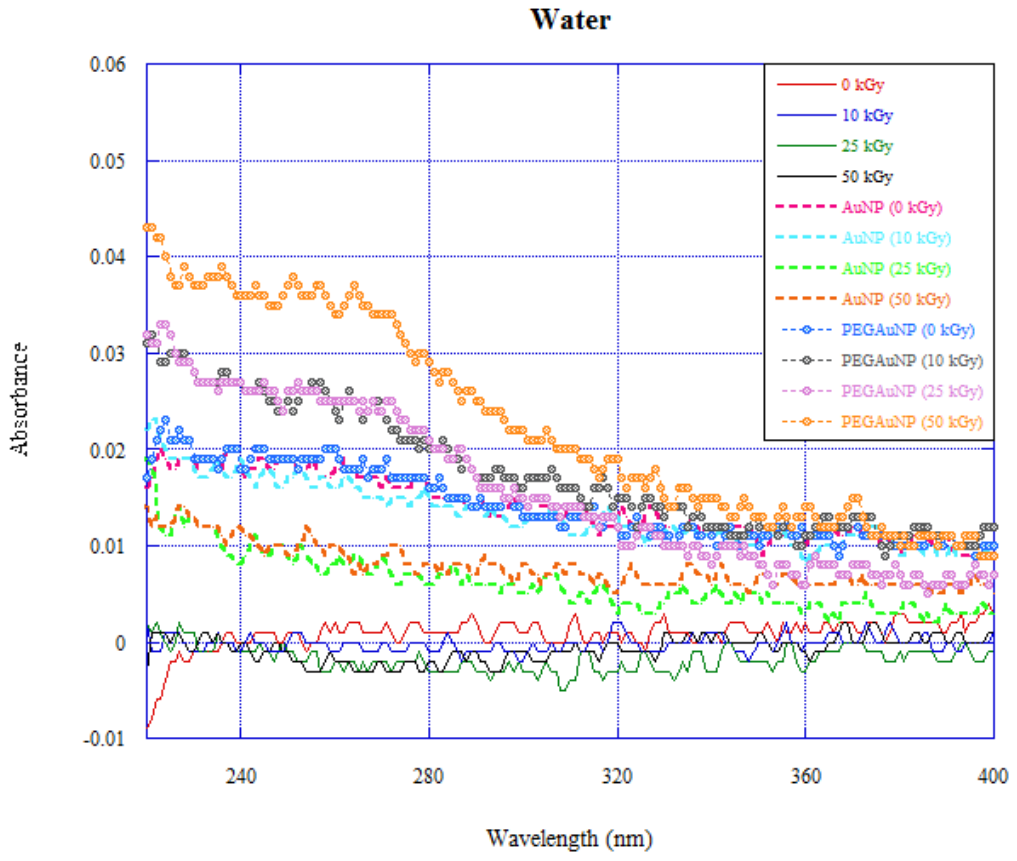

Figure A1: UV-VIS absorbance spectra for water in isolation and with AuNPs and PEG-AuNPs.

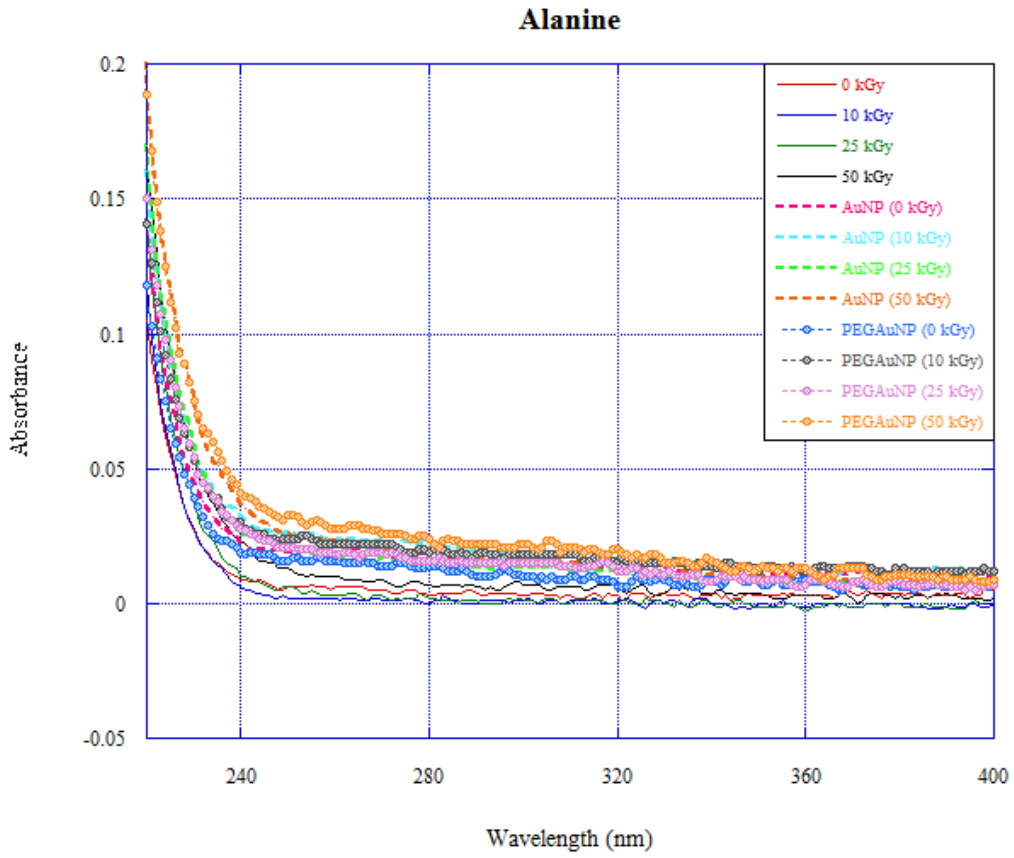

Figure A2: UV-VIS absorbance spectra for alanine in isolation and with AuNPs and PEG-AuNPs.

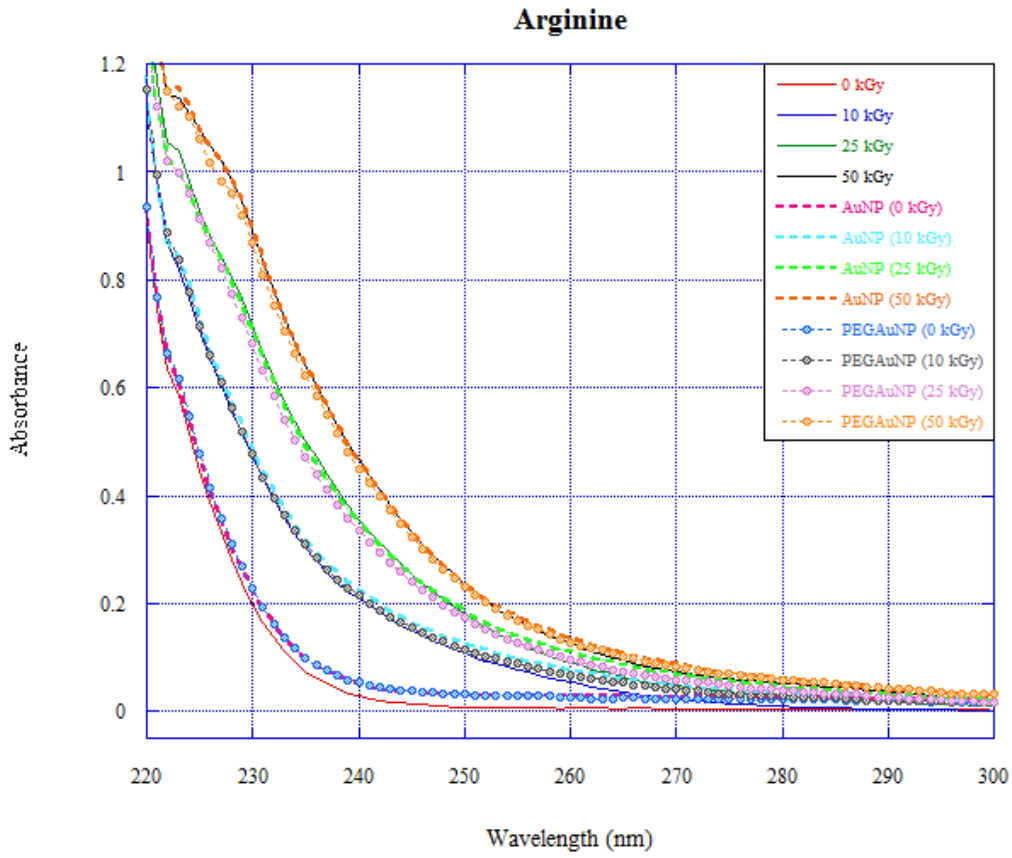

Figure A3: UV-VIS absorbance spectra for arginine in isolation and with AuNPs and PEG-AuNPs

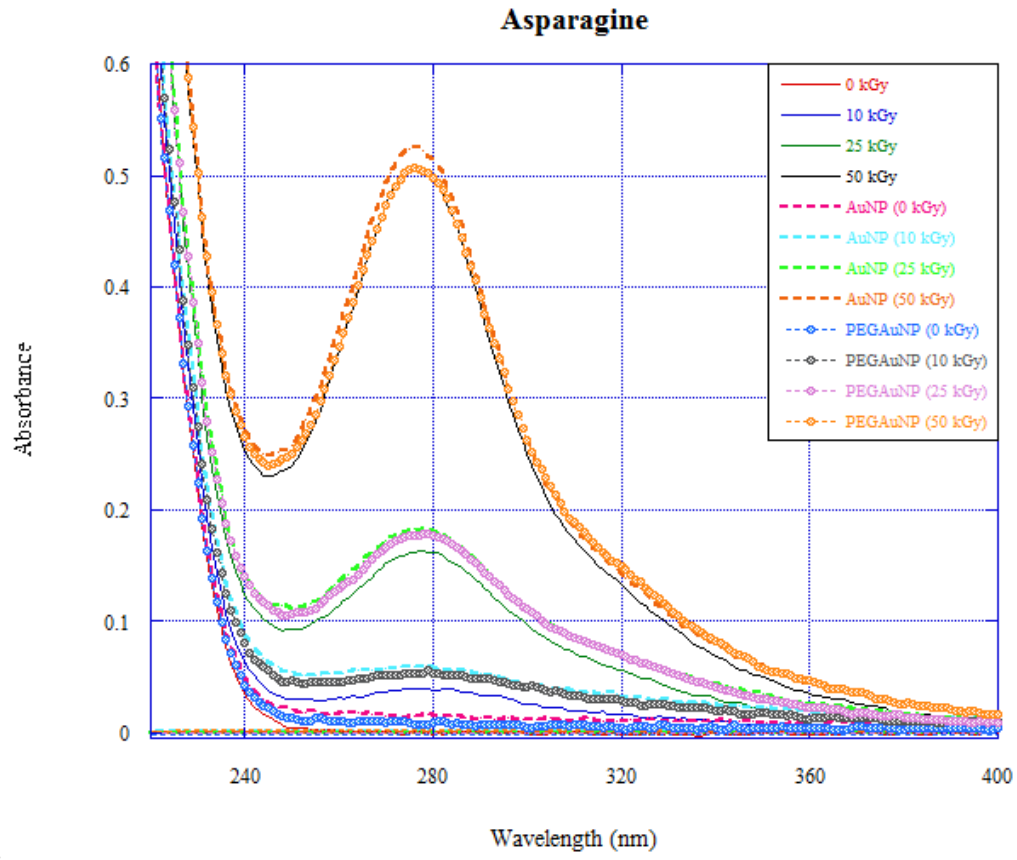

Figure A4: UV-VIS absorbance spectra for asparagine in isolation and with AuNPs and PEG-AuNPs.

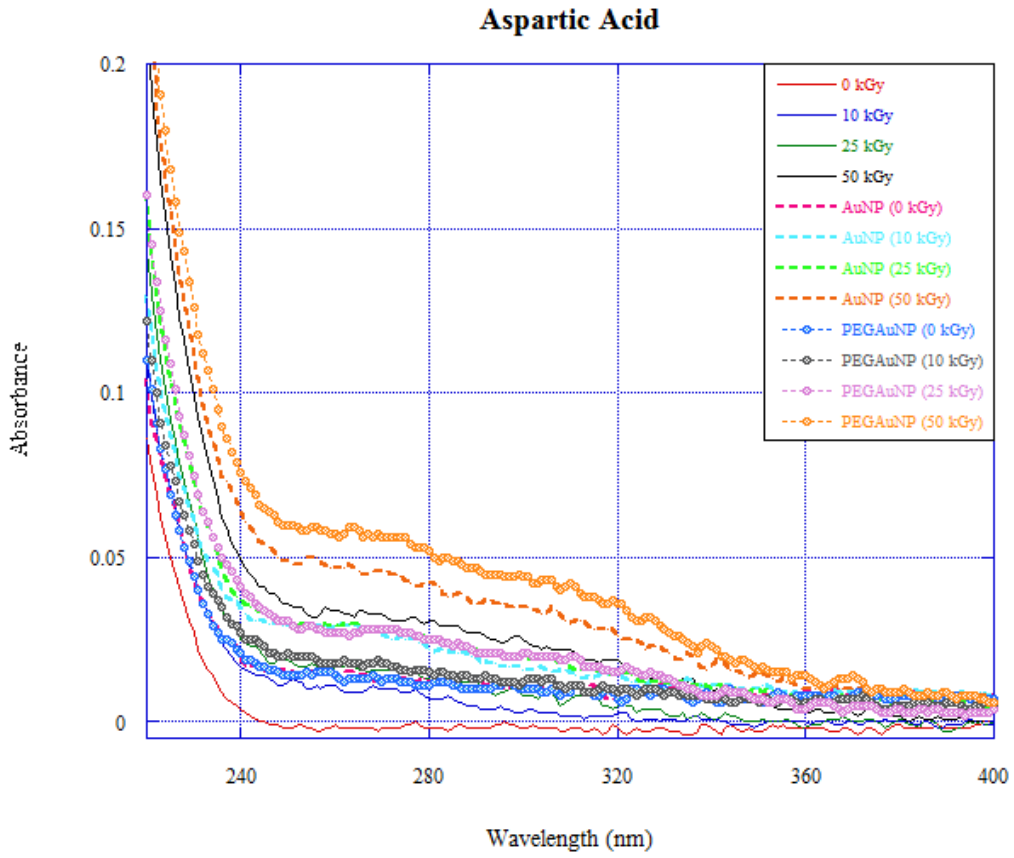

Figure A5: UV-VIS absorbance spectra for aspartic acid in isolation and with AuNPs and PEG-AuNPs.

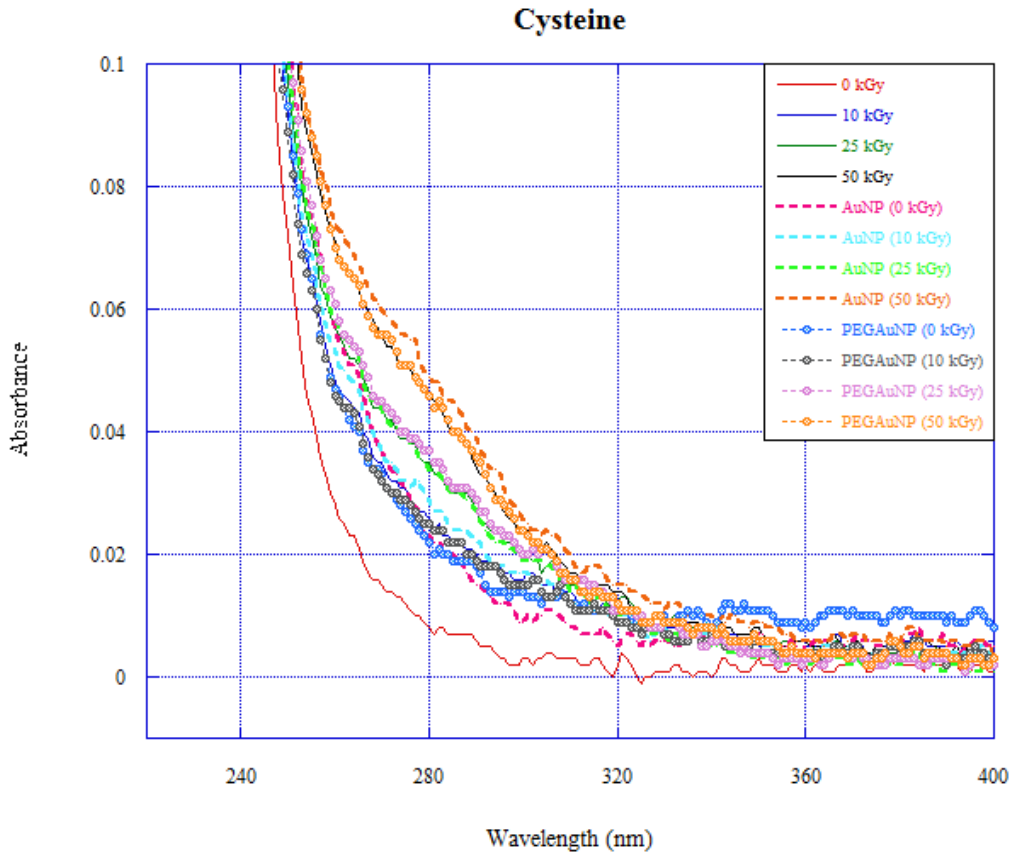

Figure A6: UV-VIS absorbance spectra for cysteine in isolation and with AuNPs and PEG-AuNPs.

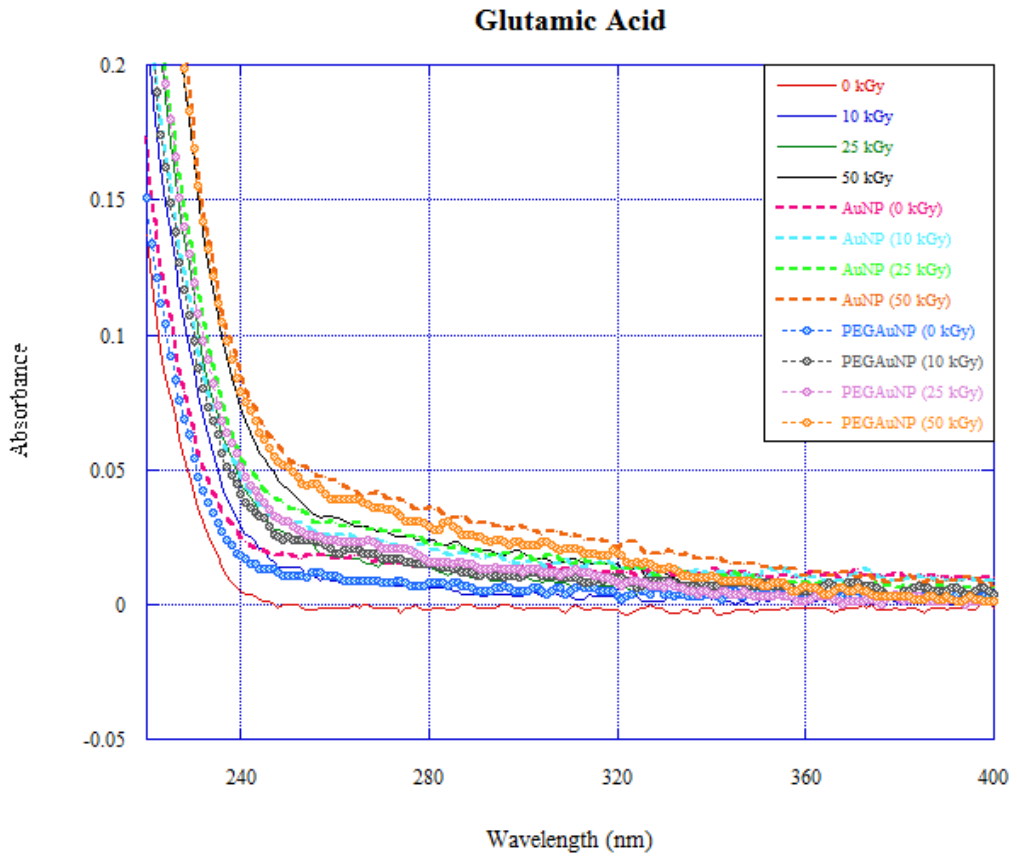

Figure A7: UV-VIS absorbance spectra for glutamic acid in isolation and with AuNPs and PEG-AuNPs.

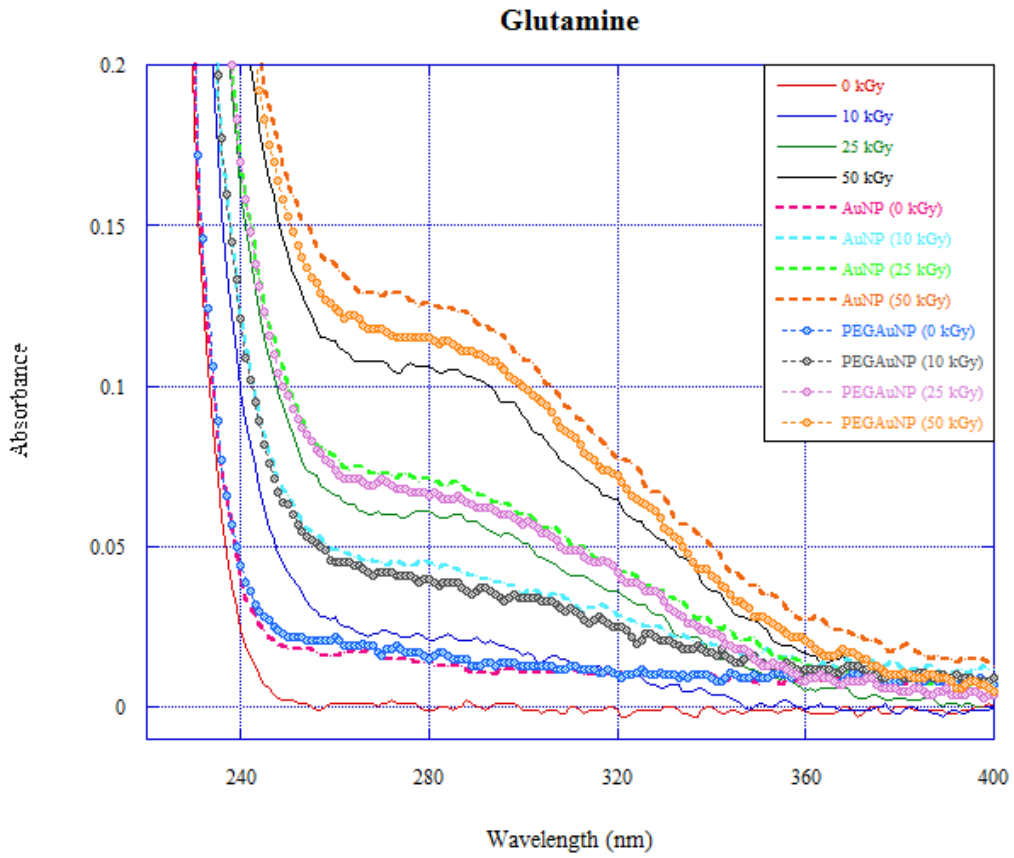

Figure A8: UV-VIS absorbance spectra for glutamine in isolation and with AuNPs and PEG-AuNPs.

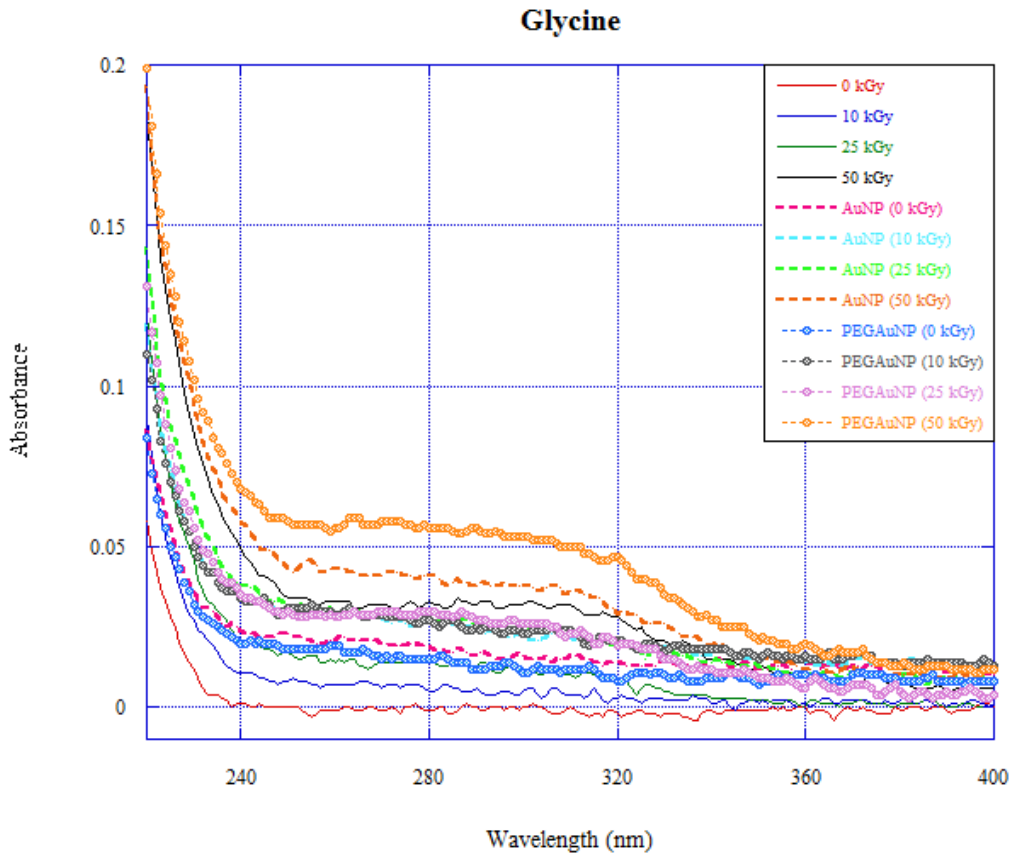

Figure A9: UV-VIS absorbance spectra for glycine in isolation and with AuNPs and PEG-AuNPs

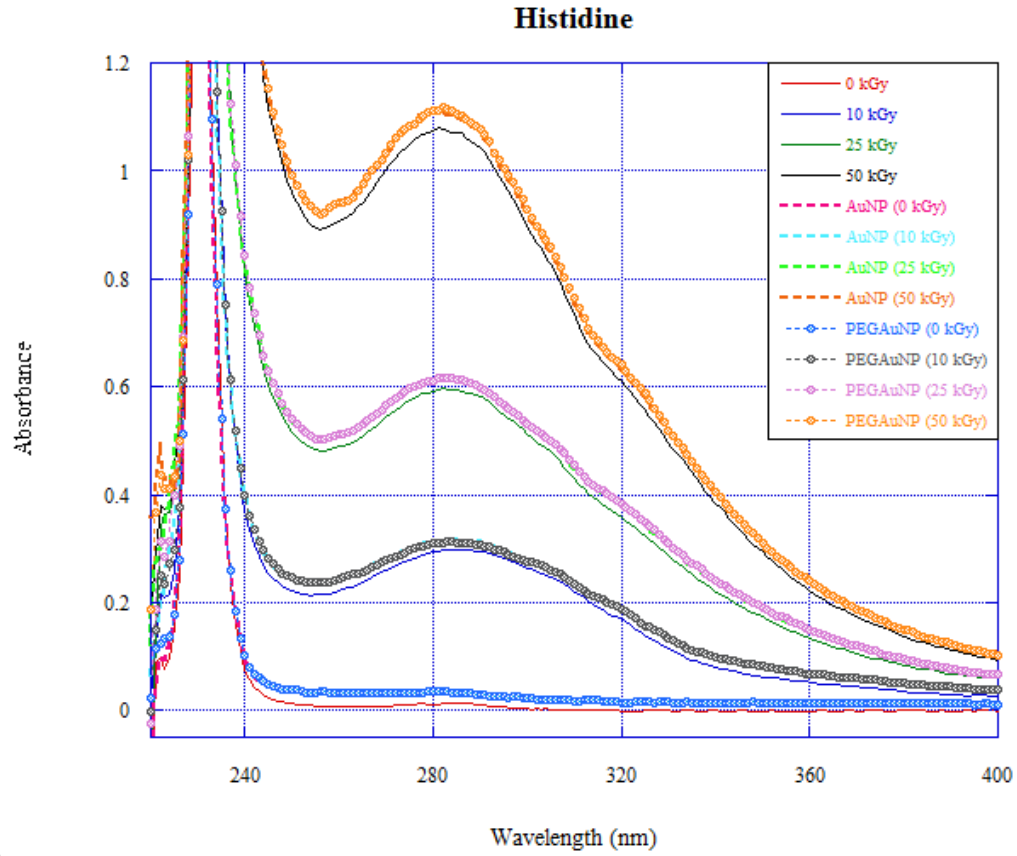

.

Figure A10: UV-VIS absorbance spectra for histidine in isolation and with AuNPs and PEG-AuNPs.

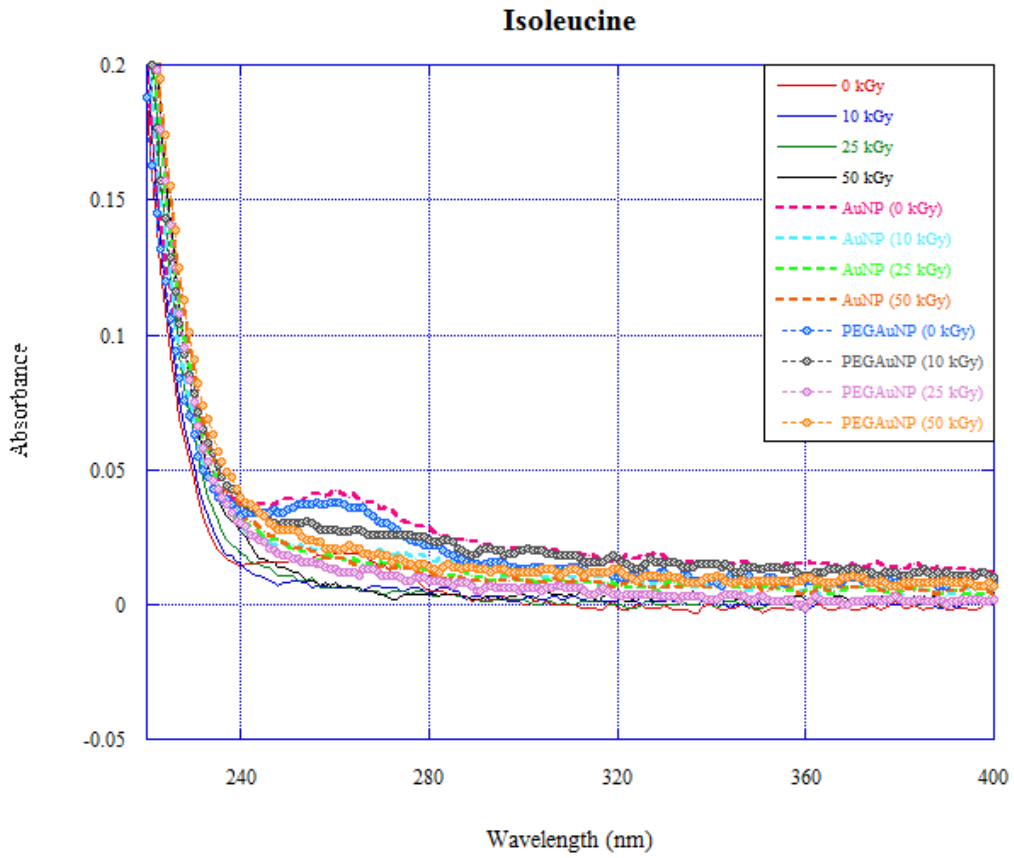

Figure A11: UV-VIS absorbance spectra for isoleucine in isolation and with AuNPs and PEG-AuNPs.

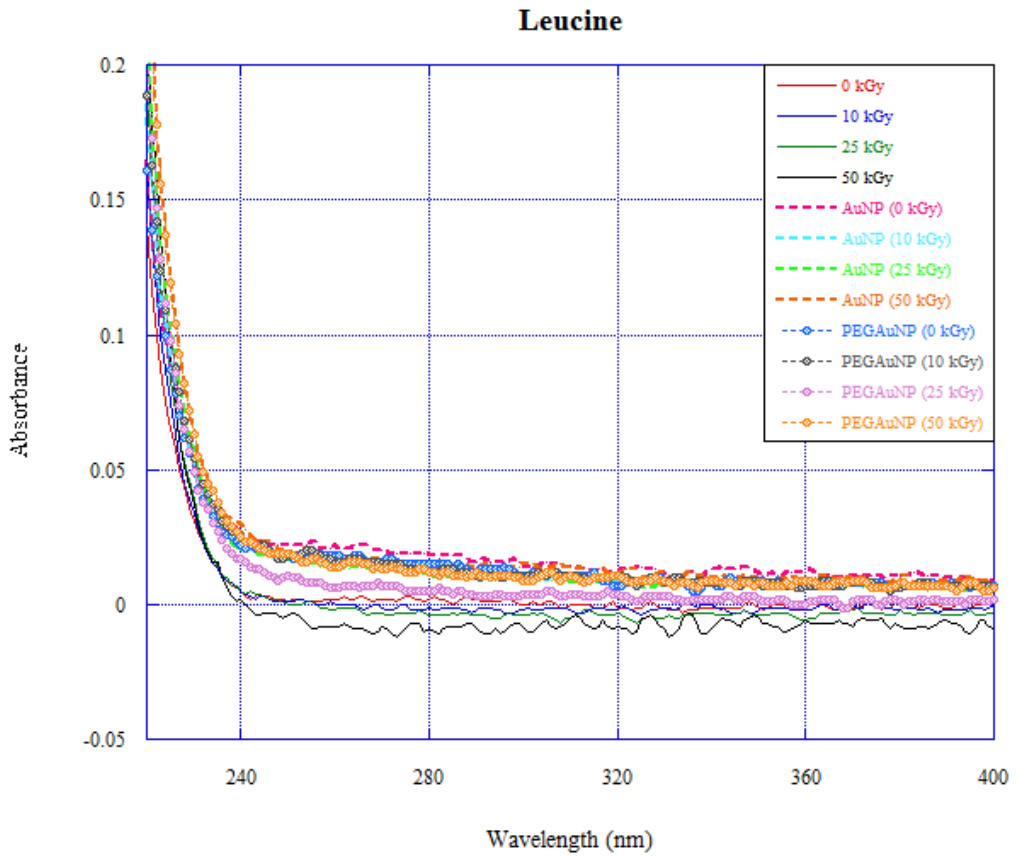

Figure A12: UV-VIS absorbance spectra for leucine in isolation and with AuNPs and PEG-AuNPs.

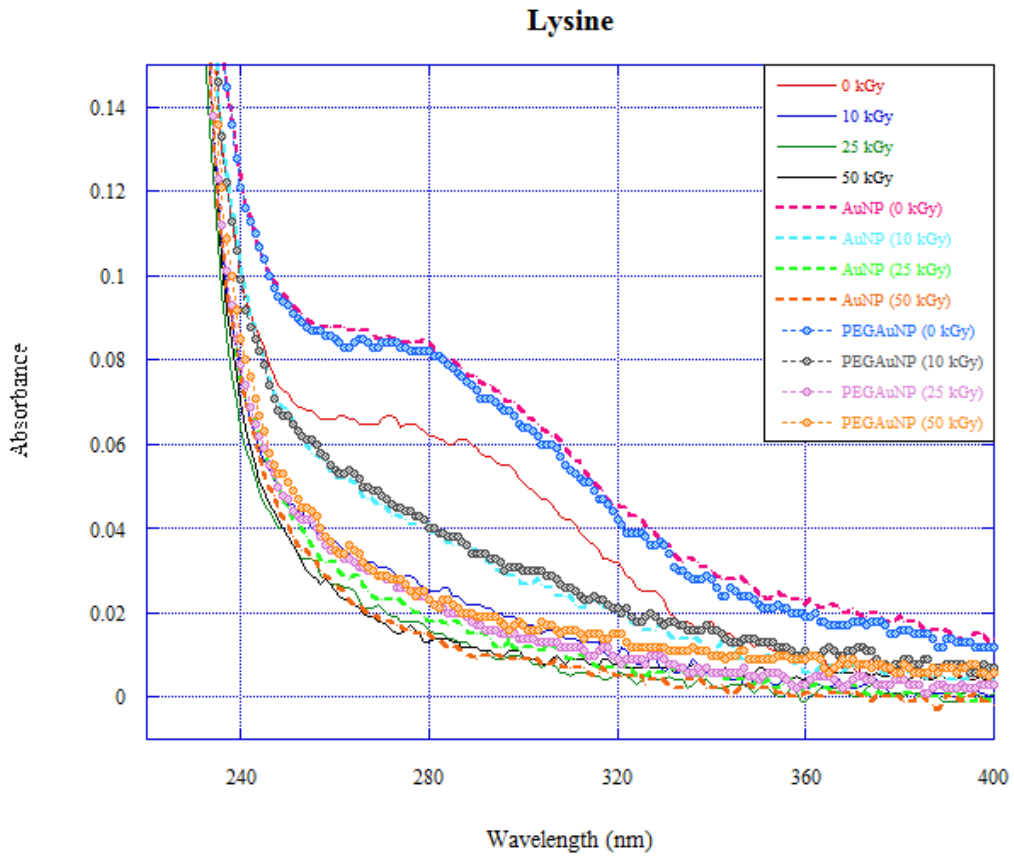

Figure A13: UV-VIS absorbance spectra for lysine in isolation and with AuNPs and PEG-AuNPs.

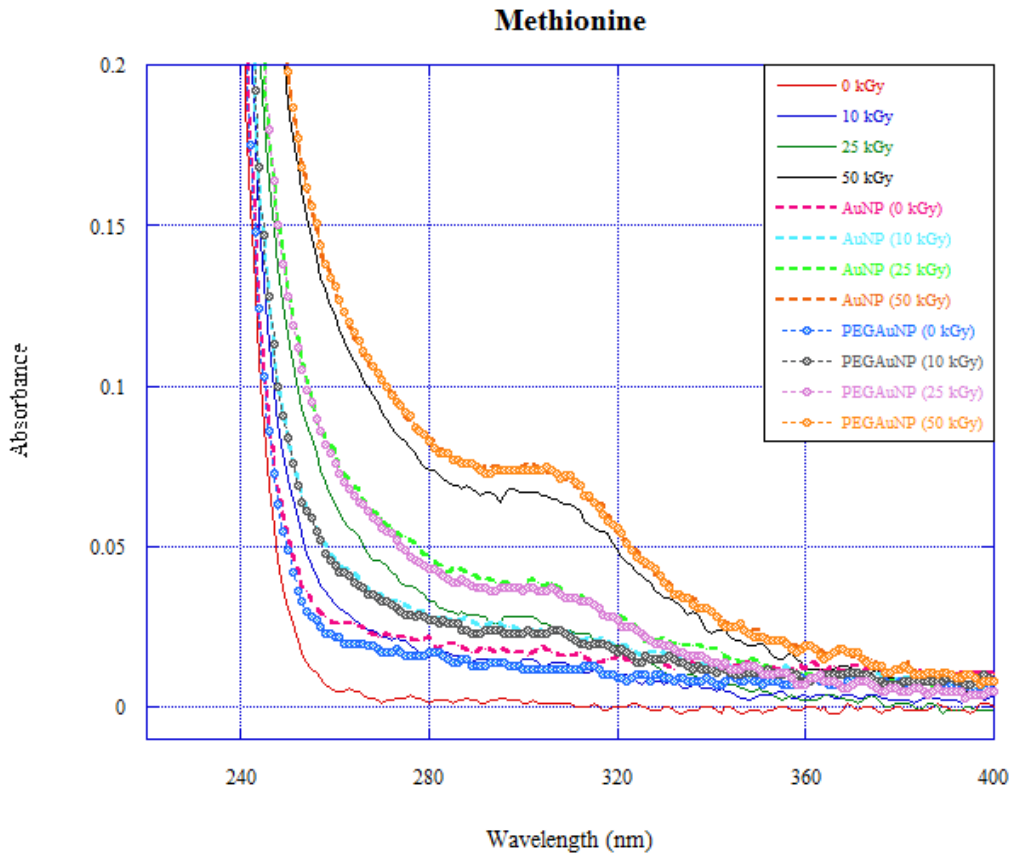

Figure A14: UV-VIS absorbance spectra for methionine in isolation and with AuNPs and PEG-AuNPs.

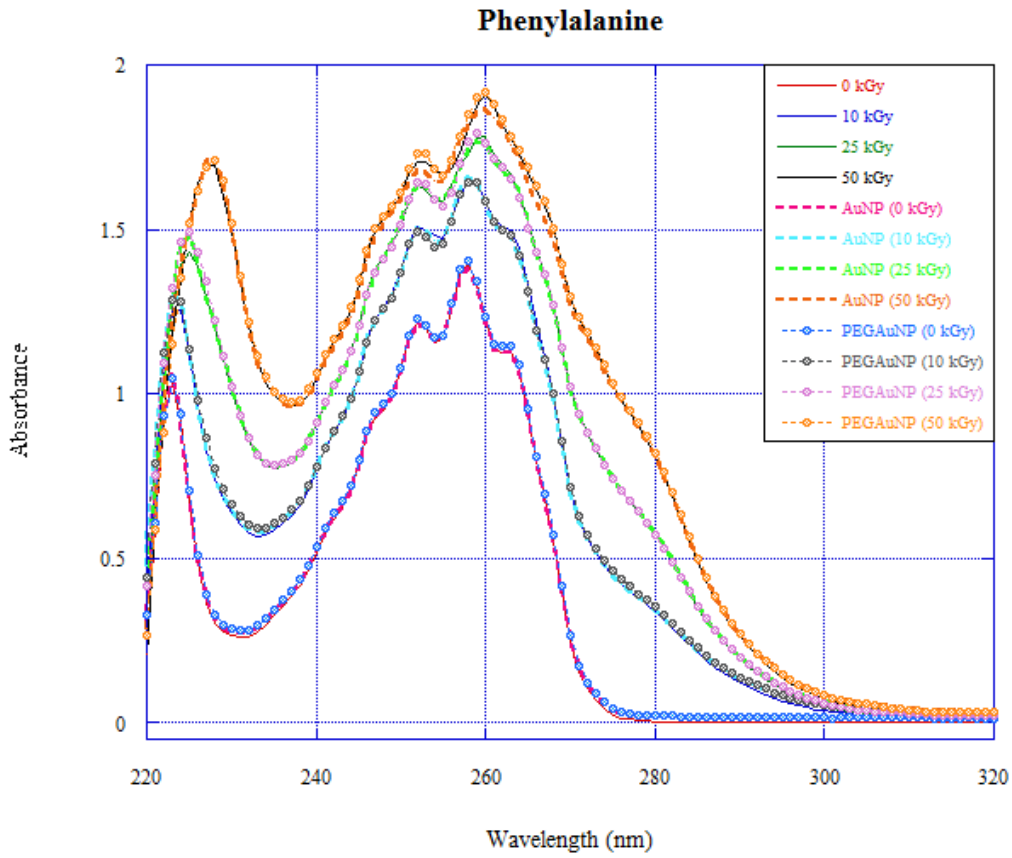

Figure A15: UV-VIS absorbance spectra for phenylalanine in isolation and with AuNPs and PEG-AuNPs.

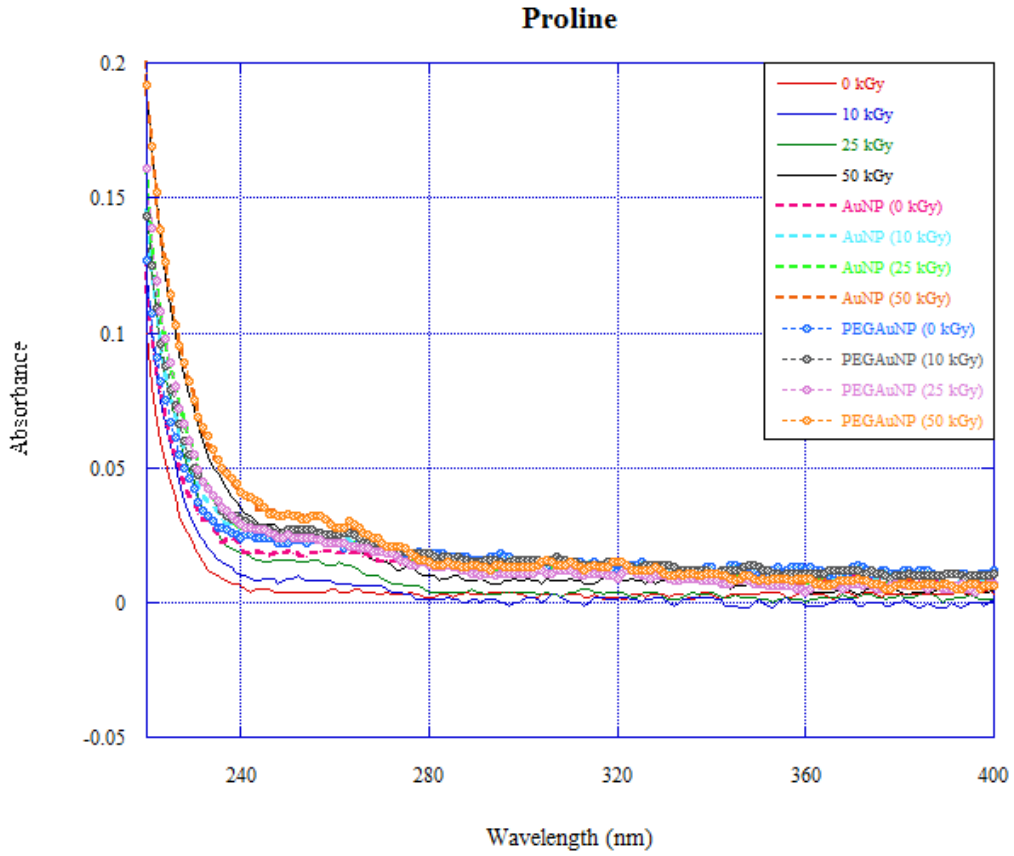

Figure A16: UV-VIS absorbance spectra for proline in isolation and with AuNPs and PEG-AuNPs.

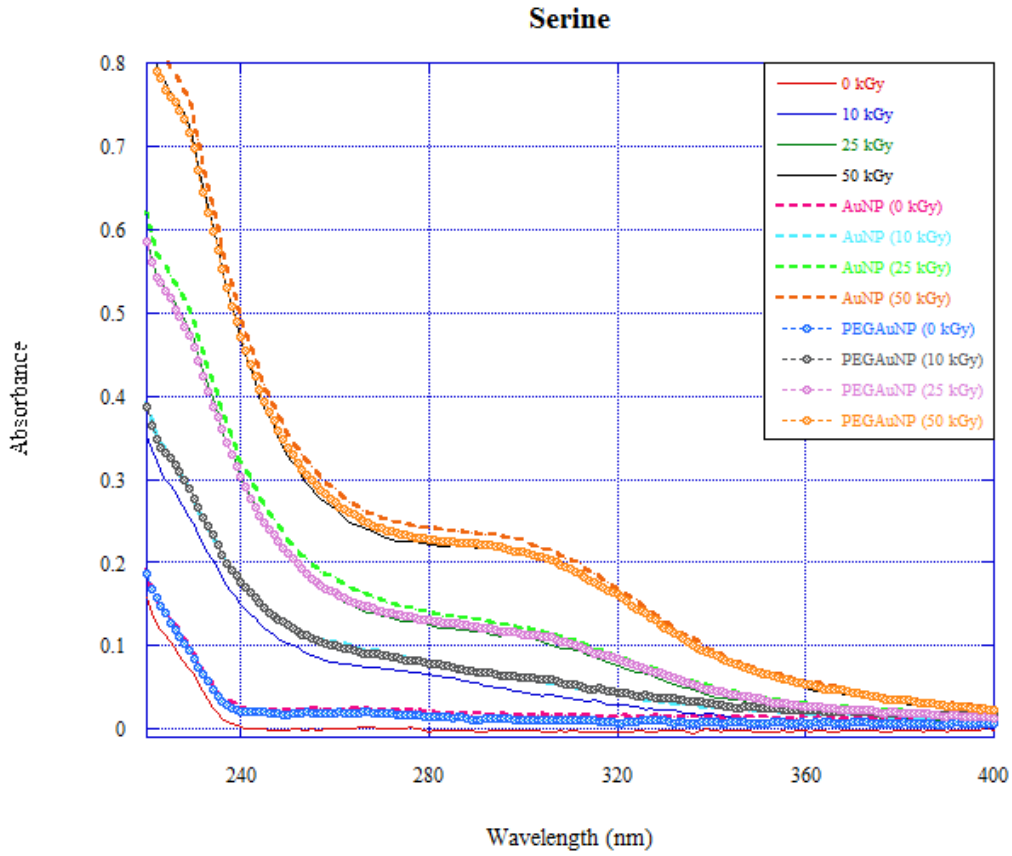

Figure A17: UV-VIS absorbance spectra for serine in isolation and with AuNPs and PEG-AuNPs.

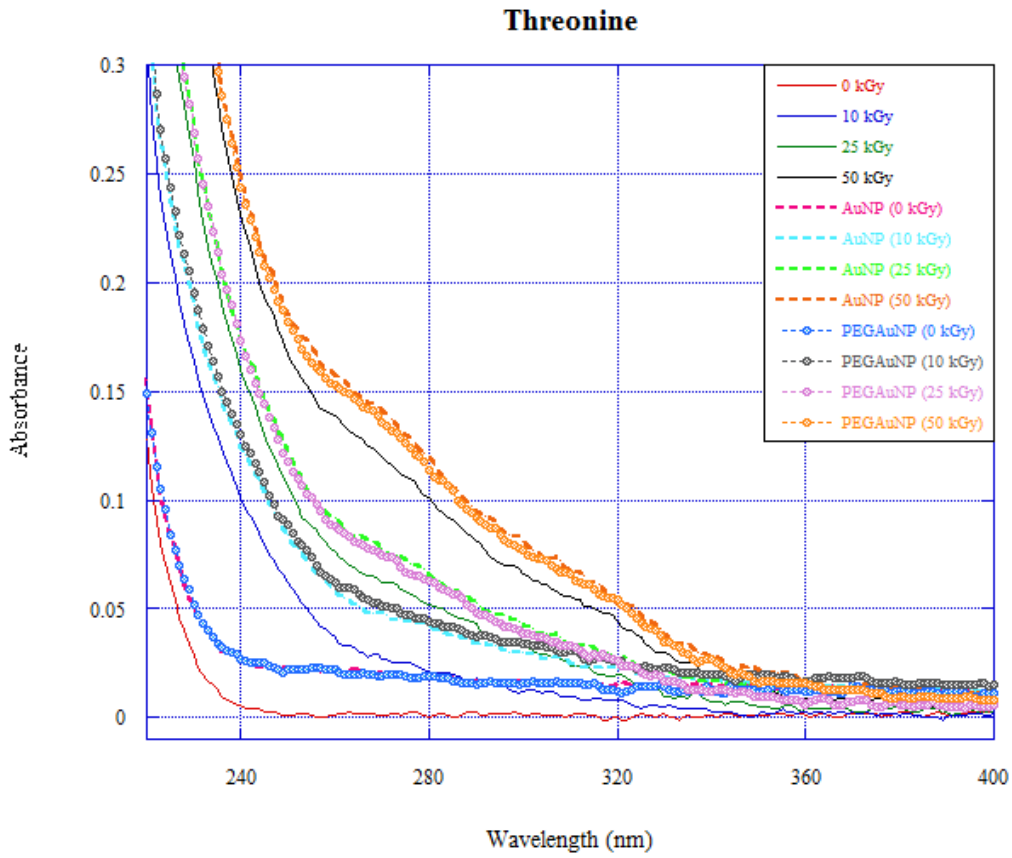

Figure A18: UV-VIS absorbance spectra for threonine in isolation and with AuNPs and PEG-AuNPs.

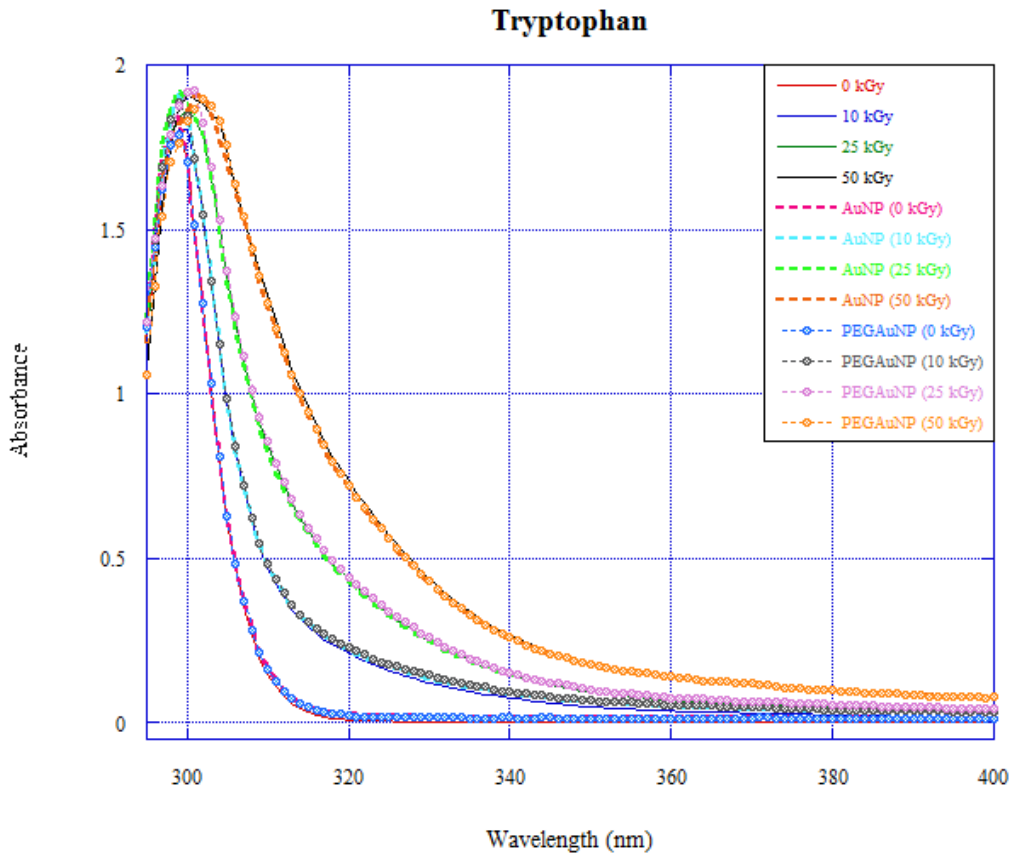

Figure A19: UV-VIS absorbance spectra for tryptophan in isolation and with AuNPs and PEG-AuNPs.

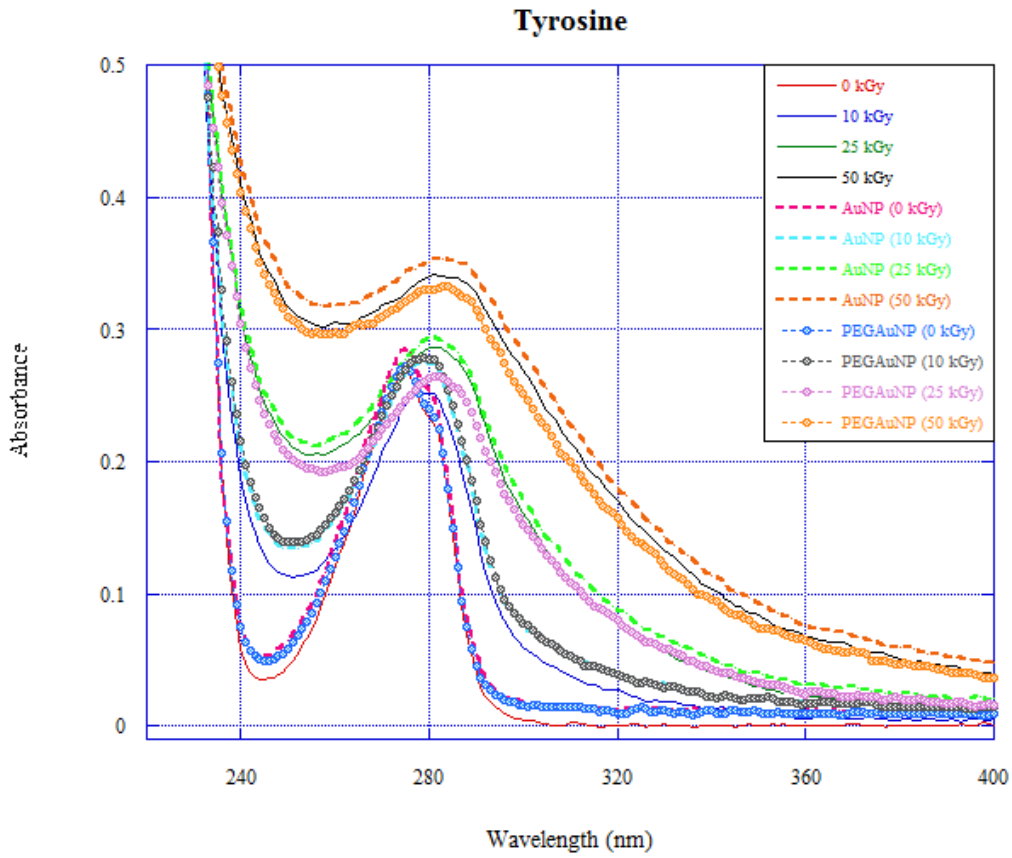

Figure A20: UV-VIS absorbance spectra for tyrosine in isolation and with AuNPs and PEG-AuNPs.

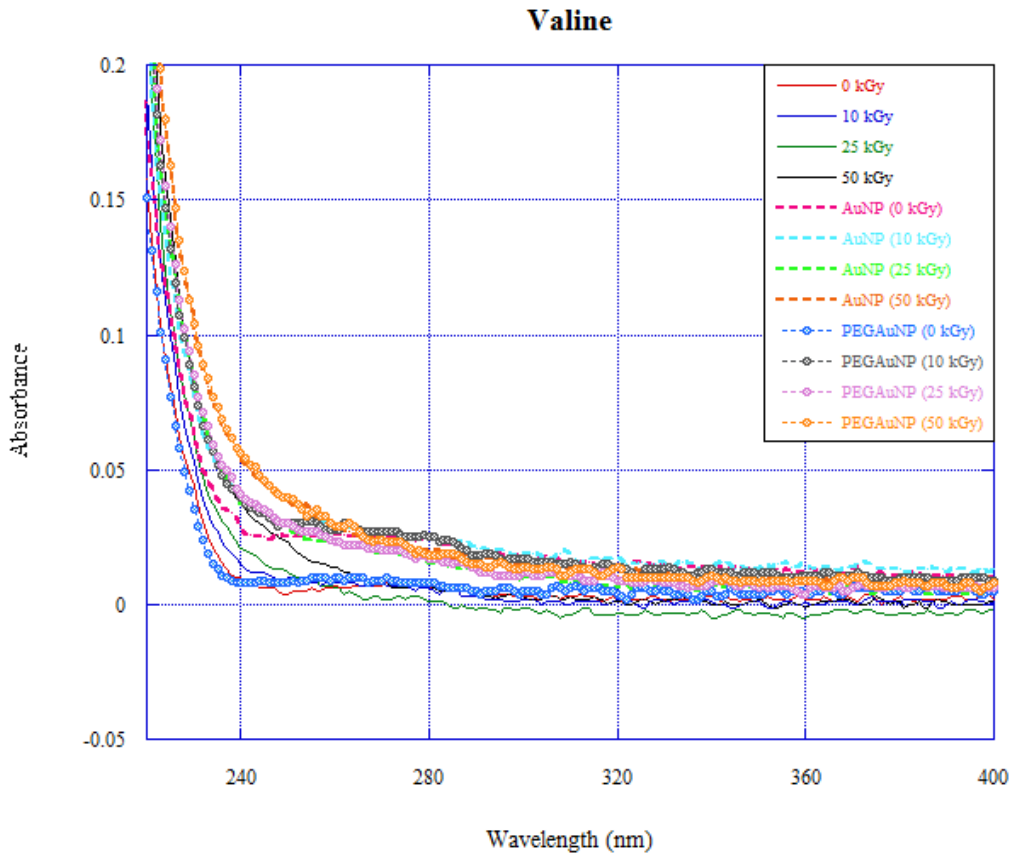

Figure A21: UV-VIS absorbance spectra for valine in isolation and with AuNPs and PEG-AuNPs.